HAWASSA UNIVERSITY

INSTITUTE OF TECHNOLOGY

DEPARTMENT OF ELECTRICAL AND COMPUTER ENGINEERING

"DETECTION, CLASSIFICATION AND MITIGATION OF POWER QUALITY DISTURBANCE: A CASE STUDY ON THE 15KV DISTRIBUTION FEEDER 6(R4-G5) AT HAWASSA SUBSTATION"

MSc. THEISS

BY: - DAWIT DABA

HAWASSA UNIVERSITY, HAWASSA, ETHIOPIA

MARCH, 2025

“DETECTION, CLASSIFICATION AND MITIGATION OF POWER QUALITY DISTURBANCE: A CASE STUDY ON THE 15KV DISTRIBUTION FEEDER 6(R4-G5) AT HAWASSA SUBSTATION”

BY: - DAWIT DABA

MAJOR ADVISOR: DR. SOLOMON MAMO (PHD)

CO-ADVISOR: MR. TESEFAHUN MOLA (MSC.)

A THESIS SUBMITTED TO THE DEPARTEMNT OF ELECTRICAL AND COMPUTER ENGINEERING,

HAWASSA INSTITUTE OF TECHNOLOGY, SCHOOL OF GRADUATE STUDIES

HAWASSA UNIVERSITY, HAWASSA, ETHIOPIA

IN PARTIAL FULFILLMENT OF THE REQUIREMENTS FOR THE DEGREE OF MASTER OF SCIENCE IN POWER SYSTEM AND ENERGY ENGINEERING

MARCH, 2025

Hawassa University

Institute of Technology

Department of Electrical and Computer Engineering

School of Post Graduate Studies

Approved by Board Examiners

We under the signed board of examiners of the final open defense by Dawit Daba have read and evaluated thesis entitled "Detection, Classification and Mitigation of Power Quality Disturbance: A Case Study on the 15kv Distribution Feeder 6(R4-G5) at Hawassa Substation" and examined the candidate. Therefore, to clarify the thesis has been accepted in partial fulfillment of the requirements for the degree.

Dr. Solomon Mamo	_____	_____
Main advisor	signature	date
Dr. Teshome Lindi	_____	_____
Internal Examiner	signature	date
Dr. Yeshitila Shiferawu	_____	_____
External Examiner	signature	date
Mr. Abenezer Bekele	_____	_____
Chair holder	signature	date
Mr. Dejene Hurisa	_____	_____
Faculty dean	signature	date
_____	_____	_____
SGS approval	signature	date

Final approval and acceptance of the thesis is contingent up on the submission of the final copy of the thesis to the school of Graduate studies (SGS) through the department Graduate committee (DGC) of Electrical and Computer Engineering.

Stamp of SGS: _____

Declaration

I undersigned, hereby declare that this thesis is my original work and has not been presented for a degree in this or any other university, and all source of materials used for this thesis has been fully acknowledged.

All examiners' comments are duly incorporated.

Name: Dawit Daba Signature: _____ Date: _____

Place: Hawassa Institute of Technology, Hawassa University, Hawassa, Ethiopia

This is to certify that the statement made above by the candidate is true to best of my knowledge and this thesis has been submitted for examination with my approval as university advisor

1. Dr. Solomon Mamo		26/02/2025
Major advisor Name	signature	date
2. Mr. Tesfahun Mola	_____	_____
Co-Advisor Name	signature	date

Acknowledgement

I want to begin by thanking God and the Virgin Mary for providing me with the courage and encouragement I needed to finish this job. Next, I want to thank Dr. Solomon and teacher Tesfahun for their commitment and advice in supporting my thesis on the identification, categorization, and mitigation of power quality. Throughout the thesis process, their knowledge and assistance were crucial, and I am appreciative of their guidance and support. I appreciate all of your efforts and dedication to my professional and academic growth. Next, I would like to thank Mr. Yalew, the South One Region's Substation Maintenance and Operation Manager, for his assistance in providing the data and information I needed for my thesis. I am really grateful for the office's assistance during the data collection stage. Finally, I would want to express my gratitude to all of my family members, Hawassa number three customer service teams, and friends who helped me out either directly or indirectly and who wish me luck.

Abstract

Modern power systems face several difficulties due to power quality disturbances, such as voltage sags and swells, which call for effective detection, classification, and mitigation techniques. In order to fully address these problems, this study offers an integrated strategy that combines modern machine learning methods with optimization techniques. Artificial Neural Networks (ANN) trained and refined with MATLAB's Classification Learner Toolbox are used for detection and classification after features are extracted from voltage/current signals. This thesis was carried out on one of the Hawassa Feeder-6 (R4-G5) 15 kV distribution feeders utilizing distribution network analysis and MATLAB simulation. The purpose of power flow analysis is to ascertain the active and reactive power flows on the distribution lines, as well as the voltage magnitude and phase angle at each bus (node) in the system. Power quality disturbances are divided into four distinct wavelet filter levels using Debechesh-4 (Db-4). This enables the improvement of an approximate and detailed coefficient distribution in addition to the extraction of features such as the mean, maximum, and lowest values of the disturbances for power quality disruptions. The classification efficacy of neural networks (ANN) and support vector machines (SVMs) is 100%. Finally, a dynamic voltage restorer (DVR) is positioned optimally using the Grasshopper Optimization (GOA) techniques. Power loss decreased from 1913.3 kW (active) and 1202.4 kVAR (reactive) to 295.534 kW and 261.803 kVAR when GOA was used, and the voltage profile was increased from 70% to 98.5% and lowered the voltage swell from 110% to 98%, and also, by applying different kinds of faults, easily tested the voltage sag and swell by using DVR integrated with wavelet transforms algorithm. This reduces the possible influence on delicate systems and equipment while simultaneously enhancing the power supply's quality.

Key words: ANN, GOA, PSO, Power Loss Reduction, WT

Contents

List of Figure

List of Table

List of Abbreviations

ANN	Artificial Neural Network
D-STATCOM	Distribution Static Compensator
DVR	Dynamic Voltage Restorer
DWT	Discrete Wavelet Transform
EEP	Ethiopian Electric Power
EEU	Ethiopian Electric Utility
EMD	Empirical Mode Decomposition
EN	European Standard
FACTS	Flexible AC Transmission System
FFNN	Feed Forward Neural Network
HSA	Hilbert Spectral Analysis
IEC	International Electro technical Commission
IEEE	Institute of Electrical and Electronics Engineers
IGBT	Insulated Gate Bipolar Transistor
MRA	Multi-Resolution Analysis
PCC	Point of Common Coupling
PLL	Phase Locked Loop
PQ	Power Quality
PQDEs	Power Quality Disturbance Events
PWM	Pulse Width Modulation
SCADA	Supervisory Control and Data Acquisition
PU	Per Unit

Chapter One
Introduction

1.1. Background

The increasing use of sensitive electronic devices and the rise in nonlinear loads have made power quality a critical issue worldwide. In developed nations, power quality disruptions are meticulously monitored and addressed using advanced techniques. According to the IEEE Standard, power quality involves powering and grounding electronic equipment appropriately and maintaining bus voltage at the rated voltage and frequency (Mohammed, 2020). Power quality disturbances, such as voltage, current, and frequency variations, can cause equipment malfunctions and failures [1]. To maintain power quality at acceptable levels, standards specify permissible limits for various performance indices and provide guidelines for consumers, manufacturers, and utilities [2]. Despite ongoing efforts to upgrade urban distribution networks in cities like Addis Ababa and Power outages continued to occur often and for extended periods of time in Dawa, Ethiopia (Ethiopian Electric Power, 2018).

Only 45% of Ethiopians have access to electricity, despite the country's enormous potential for both renewable and nonrenewable energy resources [2]. Ensuring the reliability of the power system, especially in handling disruptions and preserving quality, is vital. Therefore, thorough identification and categorization of disruptions are required. Developing countries like Ethiopia continue to encounter difficulties because of a lack of resources and experience, whereas wealthier countries are making progress toward real-time prediction and mitigation of power quality issues using data-driven models.

However, leveraging existing data to identify and categorize power quality disturbances, train modern algorithms, and implement mitigation strategies can provide a path forward. This study aims to develop a hybrid approach using signal processing and machine learning algorithms to detect, classify, and mitigate power quality issues.

But there may be a way ahead by using the data that is already available to classify and identify power quality issues, develop cutting-edge algorithms, and put mitigation plans into action. The goal of this research is to use signal processing to create a hybrid strategy and use machine learning methods to detect, classify, and alleviate power quality concerns.

The factory stated frequent equipment failures, such as looms that suddenly reset. Motor overheating results from voltage sags (down to 160V) during peak hours (4–8 PM). Variable frequency drives (VFDs) can cause harmonic distortions that interfere with control systems. Outages of two to three hours each day result in material waste and 15% output losses [3].

The expected yearly losses from equipment repairs, missed deadlines, and downtime are $250,000. An assessment of power quality found Variations in voltage: ±20% off of the nominal value (above IEEE 1159 standards). Harmonics Total Harmonic Distortion (THD) of 12% in phases (beyond IEEE 519's 8% maximum). Inductive loads (motors) are the cause of the low power factor of 0.75, which increases reactive power penalty. Grid instability: Overloading during periods of high demand and inadequate distribution infrastructure. The main causes include aging transformers and undersized cables in the industrial area, a lack of harmonic filtering and power factor correction, and grid congestion brought on by fast urbanization and poor maintenance [17].

Solutions that have been put into practice are Correction for power factor Capacitor banks were installed, utility penalties were decreased, and PF was raised to 0.95. Voltage stabilization was implemented, automated voltage regulators (AVRs) were connected to vital equipment, and a 500kVA diesel generator was used for backup power during outages. Long-Term Harmonic Filter Upgrades at VFD connecting sites, THD was lowered to 5% via passive filters. Workshops for staff training on energy conservation, equipment upkeep, and renewable integration using a 200kW roof top solar PV system with battery storage to reduce reliance on the grid during dry spells. Most rural communities in Nigeria are dependent on the national grid's erratic and unpredictable power supply. Power quality problems such as voltage sags, harmonics, and electrical noise have resulted from this. Certain problems have made it more difficult for small enterprises and farming to expand in certain areas. The Nigerian government launched the Rural Electrification Agency (REA) initiative to solve these issues with electricity quality. The program's goal is to give rural areas access to off-grid power. Micro-hydroelectric power plants, small-scale wind turbines, and solar mini-grid systems are some examples of these solutions. Rural communities now have better power quality and dependability because of these decentralized power sources, which have increased agricultural output and allowed small enterprises to run more effectively [17].

1.2 Statement of Problem

Voltage problems like sags and swells are becoming more and more problematic for Ethiopian Electric Utilities. In feeder six (R4-G5) of the Hawassa electric power distribution network, there is a notable voltage sag of 70%, a voltage swell of 1.315% and 28.685% normal voltage from base case of load flow . Non-linear loads, extended feeder coverage lengths, and occasionally various fault types are the main causes of these interruptions. Depending on the sensitivity of their equipment as well as the magnitude and length of the voltage variations, different consumer types may experience distinct effects from voltage sags and swells. Here are some more specific instances of how residential, business, and industrial consumers may be affected by voltage sags and swells. Voltage sags experienced by residential consumers can result in flickering lights, malfunctioning or reset electronic gadgets, and less efficient appliances. For homeowners who depend on delicate electrical devices for work or play, this might be very inconvenient. By subjecting them to higher-than-normal voltage levels, voltage swells can harm electronic gadgets like PCs, TVs, and game consoles. For homeowners who are not sufficiently protected by surge suppressors, this may result in expensive repairs or replacements. Commercial consumer voltage sags have the potential to interfere with business operations in places like restaurants, retail stores, and small offices. For instance, a drop in voltage may result in refrigeration units failing, cash registers malfunctioning, or credit card machines resetting, which could cost businesses money and possibly annoy customers. In business settings such as server rooms, data centers, and manufacturing facilities, sensitive equipment might sustain harm from voltage swells. For companies that depend on constant functioning, a spike in voltage could result in data corruption, equipment failure, and expensive downtime. Industrial sags in consumer voltage can significantly affect industrial processes that need careful monitoring and control. A voltage drop, for instance, may cause sensors to fail, motors to halt, or control systems to become unresponsive, which could lead to production delays and possible product flaws. In industrial environments like power plants, refineries, and chemical processing facilities, sensitive equipment can sustain harm from voltage swells. An increase in voltage poses major safety risks as well as possible environmental dangers since it can cause electrical fires, insulation failure, and equipment overheating.

1.3 Objectives of this Study

1.3.1 General Objective:

To develop an effective method for detecting, classifying, and mitigating power quality disturbances in the 15kV Distribution Feeder 6 (R4-G5) of the Hawassa Substation, using advanced signal processing, machine learning, and optimization techniques to improve power system reliability and stability.

1.3.2 Specific Objectives:

- To detect and classify power quality disturbances using wavelet transforms (WT) and the Classification Learner toolbox.
- Improve the voltage level of the existing system from 70% (0.714pu) to 95% (0.95pu).
- Compare GOA with the PSO technique.
- Design and testing of DVR with Simulink.
- Cost-benefits analysis by reducing the annual power loss.

1.4 Scope of this thesis

The goal of this thesis is to identify, categorize, and address power quality issues in the Hawassa electric power distribution system. Feeder 6 (R4-G5) is connected to substation one is the main focus. The study determines the origins and consequences of power quality issues such as voltage sag and swell. For this thesis, feeder 6 was given priority above other feeders because of the following important factors: historical information on disruptions in comparison to residential or mixed-use feeders, utility records indicated that feeder 6 saw the most frequent voltage sags and swells (15–20 incidents per month). This was in accordance with industrial complaints of feeder 6 infrastructure equipment failures (such as oversized wires and obsolete transformers), which increased line impedance and exacerbated voltage reductions during peak demand (4–8 PM) and long-distance coverage (about 87 km). Additionally, it models mitigation techniques that improve the power supply's quality by combining DVR and discrete wavelet transform.

Chapter Two

Literature Review

2.1 Introduction

In order to improve the bus voltage profile of power system networks, this thesis describes the research that will be done on power quality disturbance detection, categorization, and mitigation using the best possible DVR location and sizing as well as the Matlab toolbox. The ideas of small signal and large signal disturbance of power systems are examined, along with descriptions of related research studies that have been published in the technical literature.

2.2 Summary of Some Researcher Studies

Studying power quality and related disturbances requires quick, accurate, and prudent disturbance detection and classification. To properly examine and deal with these disruptions, it is critical to categorize them according to particular standards. The impact of power quality disruptions depends on the frequency and intensity of signals. The intricacy of power system operations frequently causes problems for analysts and monitoring algorithms when it comes to ordinary data analysis [1].

To comprehend these occurrences, a sophisticated algorithm for feature extraction, detection, and classification is required. Mathematical solutions for signal management in power systems are provided by artificial intelligence algorithms in conjunction with signal processing. The ability of different methodological approaches to identify, categorizes, and mitigates power quality issues are examined in this study.

It is the most basic and initial stage in identifying and categorizing power quality issues. Depending on the consumers, different power quality issues must be recognized and classified. Problems that need to be investigated include process requirements, equipment type, and the financial impact of issues; some of these concerns may affect the utility distribution system in addition to the customer's facilities [2].

The impact of automation on the electric distribution network's dependability in 2018 is examined in this article, with an emphasis on how automation of secondary substations (SS) can improve the reliability index. Availability and latency are taken into consideration when using less-than-ideal communication links during the automation process [16].

Uses four carefully selected 15kv feeders to assess the reliability of the bahir dar city distribution system. With the use of ETAP software and modified shark smell optimization (MSSO), the reliability of the distribution network indices as a whole behavior is assessed. Additionally, the researcher recommends that additional recloser be utilized in conjunction with economical methods of system improvement, such as reconnecting the system and replacing obsolete components. Distribute the load break switches and place them in strategic locations [17].

Using test and ideal switches and a 33-bus test distribution network as a test case for reorganization problems, this study explores a novel method for Distribution Network Reconfiguration Analysis under Varying Load Demands in 2017 [18].

This study presents a grasshopper optimization technique for simulated reconfiguration of the distribution circuit with the goal of minimizing power loss by leveraging grasshopper behavior. When tested on an IEEE 33-bus radially distribution system, the method yields the best results in a reasonable amount of calculation time and performs better than existing optimization strategies [19].

In order to enhance energy efficiency and grid management in distribution networks, this research suggests an optimization methodology for a combined power loss reduction technique. Reactive power compensation, transformer replacement, and line replacement are all taken into account in the plan. Experiments demonstrate that the cost-benefit ratio-based methodology successfully lowers power loss in Tianjin [29].

The implementation of particle swarm optimization (PSO) and moth flame optimization (MFO) techniques to determine the appropriate location and size of a Static Var Compensator (SVC) within a Distribution Network (DN) is covered in this study. Reducing voltage variation and power interruptions is the aim, particularly during periods of high electricity demand. The outcomes were compared to PSO results and evaluated on the Wolaita sodo radial distribution. In the distribution system, the SVC with MFA base did better [32].

The Grasshopper Optimization method (GOA), an optimization method that emulates the actions of grasshopper swarms in the wild, is presented in this study. It is used to determine the best shapes in structural optimization and is tested on CEC2005. When applied to real-world issues with unknown search spaces, the suggested technique performs better than literature-based approaches as established by real applications [34].

Table 2. 1 Summary of literature review

Authors	**Techniques**	**Strengths**	**Limitations**
Mr. Alamm et al.	Fast Fourier series Transform	Reduced computational load because there is no data testing or training	Did not study multiple disturbances. Lack of time-frequency domain representation.
K. Deepthi	DFT-Voltage Slope Detection technique	Has less computational complexity	No mitigation mechanism was considered.
Fayyaz Jandan	DWT-ANN	Included both single and multiple disturbances	No mitigation mechanism was considered.
Hen-Geul et al.	WT-based orthogonal algorithm	Effective, fast, and perfect in detecting high-impedance faults	Did not consider the classification and mitigation of disturbances.
M. Ismail et al.	DWT-ANN	properly classified the training and tested signal	Only a few PQDs were considered and no mitigation mechanism was used.

2.2.1 Researches gap and improvement

The weaknesses of the above literatures are précised as follows:

- Most of them primarily concentrate on classifying and detecting power quality disturbance but often overlook developing practical mitigation strategies to address them effectively.
- Cost-benefit analysis not considered in the researches.
- A detail load flow analysis did not consider.

This thesis fills the gap of the above researcher by using different types of classifier to identify voltage sag, swell and normal conditions, detection techniques like voltage monitoring, wavelet transforms, and neural network classify events by magnitude, duration, and waveform distortion. The optimal placement of dvr and load flow analysis is used to identify week network nodes with frequent voltage issues and cost-benefit analysis for long term saving by reducing the power loss of the feeder 6.

2.3 Theoretical Background

2.3.1 Classification of Power Quality disturbance

The power quality valuation method offers a comprehensive context that covers all the elements that may be desired to identify and classify power quality disruptions. The most common power system issues identified by a general-purpose power quality evaluation are included in this study. The power quality disturbance investigation approach employed in this thesis contains the next phases.

2.3.1.1 Classifying the voltage sag and swell and extracted feature

It is the most basic and initial stage in identifying and categorizing power quality issues. Depending on the consumers, different power quality issues must be recognized and classified. Problems that need to be investigated include process requirements, equipment type, and the financial impact of issues; some of these concerns may affect the utility distribution system in addition to the customer's facilities [2].

Power quality problems have existed since the development of electric power, and there are several solutions to address these problems. Although many pieces of equipment are designed to work well even when there are voltage sag, swell disturbing, the following factors have made consumers much more aware of power quality problems [2].

An early phase in the method is the classifying of power quality issues, which comes before the detection, classification, and mitigation approaches. The next steps involve employing an

artificial neural network algorithm in conjunction with the wavelet transform to detect and classify disturbance signals.

2.3.2 PQDs Detection through Signal Processing Methods

Signal processing is concerned with evaluating, varying, and combining signal and is used to advance transmission, storage efficiency, and quality as well as detect components of measured signals. Analyzing, altering, and synthesizing signals is the focus of signal processing, which is also used to identify components of measured signals and enhance transmission, storage, and quality [4].

2.3.2.1 Fourier Transform (FT)

Frequency domain analysis is where the Fourier transform is most frequently used for feature extraction and detection. Although FT has been shown to be a useful technique for breaking down the components of stationary signals, it is not appropriate for analyzing non-stationary signals. Discrete Fourier transforms (DFT), Fast Fourier transforms (FFT), and short-time Fourier transform (STFT) are the three different versions of Fourier transforms (FT). Fourier transform is the basic analytical method used to define power values in IEEE Standard 1459-2010 [6].

FT is commonly used to split a signal into a sum of frequencies for stationary signals, but it is difficult to obtain time information when the signal fluctuates. For this reason, advances in Discrete Fourier Transform (DFT), which is used to detect power system disruptions, have been made. DFT is only a good algorithm for stationary PQDEs; it cannot handle variations in power quality disturbances. To detect PQDEs, another FT derivative called the Short Time Fourier Transform (STFT) can divided the error signals in to smaller pieces, all of which is considered a stationary signal. Since harmonics are one of the steady state events and produce the same discoveries as other steady-state events, the Fast Fourier Transform (FFT) is appropriate for evaluating harmonics, where it has the same conclusions that can be done by DFT, but in less time. However, due to leakage discovered by FFT [7].

The discrete Fourier transform (DFT) a sequence of *N* complex numbers $x_{n=}\ x_{0,}x_{1,\ldots..}x_{n-1}$ into another sequence of complex numbers,$(X_{k)\,=}\,X_{0,}X_{1,\ldots\ldots.}X_{N-1}$ which is defined by:

$$\mathrm{Xk} = \sum_{n=0}^{N-1} Xn.\, e^{i2\pi \frac{\mathrm{k}}{\mathrm{N}} * \mathrm{n}} \qquad (2.1)$$

2.3.2.2 Wavelet Transforms (WT)

The wavelet transform is used to analyze non-stationary signals in time and frequency domain representations. The sample frequency, the degree of decomposition and the chosen mother wavelet determine the accuracy of WT. Data events that Fourier analysis techniques would miss, like trends, breakdown points, and discontinuities, can be found using wavelet analysis. The WT method is a powerful tool for feature extraction and is crucial to PQDE discontinuity identification. The list of popular wavelet types is under. Daubechis 4 (db4), a subclass of the Daubechis wavelet class, is typically used for PQDE study due to its features that are somewhat similar to the events [7]. Baseband features are present in the frequency domain of wavelet analysis. Wavelet analysis's variable window size, which is broad for gradual changes or low frequencies and narrow for sudden or rapid changes, is its main advantage over other techniques. An effective tool for analyzing transient phenomena in power systems is the WT. In many applications, it has taken the place of Fourier analysis since it can concurrently extract information from transitory signals in the time and frequency domains. The fundamental benefit of wavelets is that they enable simultaneous localization in the frequency and time domains by utilizing fast wavelet transforms, which are incredibly computationally efficient. WT is an advanced signal-progressing technique that can be applied to power quality studies. Discrete wavelet transforms (DWT), discrete wavelet packet transforms (DWPT), and continuous wavelet transforms (CWT) are the three subcategories of WT. Signals are broken down into numerous sums of short-term waveforms, which are collectively referred to as the mother wavelet, through a process known as decomposition. WT and FT differ principally in that WT has an advantage in assessing power quality disturbances due to its availability of signal information in the time-frequency domain.

Additional information regarding signals, including the amplitude, energy level, and standard deviation, is contained in these coefficients [9].

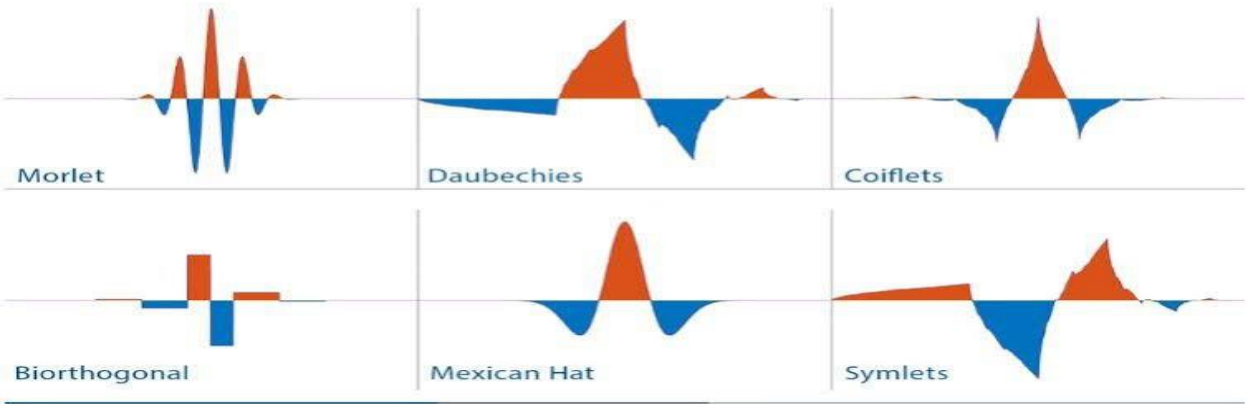

Figure 2. 1 Basic Types of Mother Wavelets

When it comes to power quality disturbance detection, WT can detect non-stationary disturbances fast. The algorithm proposed to quantify the magnitude of a single incident shows how well DWT detects voltage dips in power quality disturbances [1]. The following is the general DWT equation for signal x (k):

$$\text{DWT}(\text{m},\text{n}) = \frac{1}{\sqrt{co^m}} \sum_k x(k) \varphi \left(\frac{\text{n} - \text{kdo}co^m}{co^m} \right) \qquad (2.2)$$

Where c_o and d_o are discrete scaling and discrete translation factors, respectively, and φ is the mother wavelet. The scale and translation parameters, m and n, stand for frequency localization and temporal localization, respectively. Having fixed constant values, co = 2 and do = 1, c_o^m and $kdoco^m$ are constants. The parameter co^m produces the oscillatory frequency and length of the wavelet, whereas $kdoco^m$ credits shifting (translation) position..

To increase approximation coefficients and frequency resolution for details, decomposition is repeated up to several stages in MRA. The sample waveform under analysis is run through a half-band LP filter with an impulse response of l in MRA-based wave decomposition. In discrete time, this results in the convolution, which has the following mathematical definition:

$$(x * l)(n) = \sum^{\infty}{}_{\text{K}} = \text{-}\infty \; (k) \; (n - k) \qquad (2.3)$$

In a similar manner, a half-band HP filter can simultaneously decompose the signal. For the first level of decomposition, or down sampling by a factor of two, the HP and LP filter outputs are called detail D1 and approximation level A1, respectively. For level 2 decomposition the same HP and LP filters are applied to the derived approximation A1 coefficients, resulting in coefficients D2 and A2, respectively. The same process is used to run the A2 coefficients

through filters with the same cut-off frequency constraints, and so on. This process is commonly referred to as multi-level decomposition [11]. The following is a mathematical expression for the filter output relations:

$$(n) = \sqrt{2} \sum_k (n)(2n - k) \quad (2.4)$$

$$(n) = \sqrt{2} \sum_k h(n)\varphi(2n - k) \quad (2.5)$$

Where k denotes number of samples:-

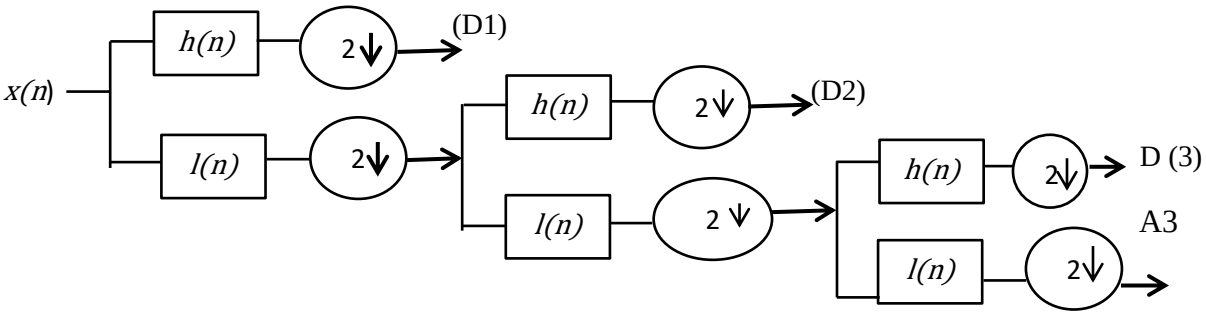

Figure 2. 2 District wavelet transforms decomposing

The approximated A_j and detail D_j coefficients are:

$$Aj+1(n) = \sum h(k - 2n)\, k\, Aj(k) \quad (2.6)$$

$$Dj+1(n) = \sum (k - 2n)\, k\, (k) \quad (2.7)$$

The mathematical relation for signal f(n) expanded about its orthogonal basis of scaling and wavelet function is shown in Equation (3.7).

$$(n) = \sum k\, A1(k)\, \emptyset(n - k) + \sum k. \sum j=1(n)\, 2^{-1/2}\, (2^j n - k) \quad (2.8)$$

By training the artificial neural network with spectral energy coordinates that have been calibrated using wavelet multi-resolution analysis. For neural network training, we employ energy coefficients from level 4 multi-resolution analyses (MRA). Input the energy of A4, D4, D3, D2, and D1 to the neural network. The aforementioned power quality disturbance examples were used to produce the target dataset and input dataset.

2.3.2.3 Stock well Transform (ST)

The Stock well Transform, created by Stock well et al., is a hybrid method for processing time-frequency signals that combines WT and STFT to produce a representation of both frequency

and time. The S-transform's inversely variable window width with frequency allows it to be used for multi-resolution analysis (MRA) of time-varying power signals. The ST's drawback is that, like the continuous wavelet transform and the short-time Fourier transform, it uses more computing resources to operate because it represents the time-frequency space redundantly [12]. Like STFT, ST localizes the complex Fourier sinusoidal signal using a window, but the width and height of the window with frequency are more like wavelets. With a 94% overall accuracy rate, the authors proposed using ST and a probabilistic neural network to detect and categorize both straightforward and complex power quality interruptions [16].

The general equation of S-transform:-

$$Sx(t,f) = \int_{-\infty}^{\infty} x(T)\lfloor f \rfloor e^{-\pi(t-T)^2} e^{-i2\pi fT} dT \qquad (2.9)$$

2.3.2.4 Hilbert-Huang Transform (HHT)

The advanced signal processing method known as the Hilbert-Huang Transform is based on a 1998 proposal by Dr. Huang for the study of non-stationary data. The two primary decomposition techniques that comprise HHT are empirical mode decomposition (EMD) and Hilbert Spectral Analysis (HSA). Using the EMD process, any non-stationary power signal with time-domain information can be divided into a number of sub-signals (Norden Huang, 1998). After then, each of these sub-signals has a distinct frequency, and EMD separates them into more specialized groupings called intrinsic mode functions (IMFs) according to their frequency.

HSA uses a time curve to calculate the instantaneous magnitude and frequency. The main advantage of HHT over FT or WT is that the EMD process acts naturally because it gets its basic functions from the signal itself. Eight power quality disturbances were then heavily used to implement HHT, and the accuracy of the system was 97.22% when WT compression was used [18]. The first IMF collected represents the highest frequency component of the extracted signal, while the lower one represents its lowest frequency component [20].

Empirical mode decomposition: - Their mean is m_1. The difference between the data and m_1 is the first component h_1:

$$x(t) - m1 = h1 \qquad (2.10)$$

Since the above-described construction of h1 should have rendered it symmetric, with all maxima positive and all minima negative, h1 should ideally meet the requirements for an IMF. A crest could turn into a local maximum following the initial sifting step. New extreme developed in this method actually disclose the right modes missing in the initial analysis. Only h1 can be regarded as a proto-IMF in the ensuing sorting procedure. H1 is handled as data in the next step:

$$h_1 - m_{11} = h_{11} \quad (2.11)$$

After repeated sifting up to *k* times, h_1 becomes an IMF, that is

$$h_{1(k-1)} - m_{1k} = h_{1k} \quad (2.12)$$

Then, h_{1k} is designated as the first IMF component of the data:

$$C_1 = h_{1K} \quad (2.13)$$

Hilbert spectrum analysis: The Hilbert transform can be used to calculate the instantaneous frequency after the intrinsic mode function components have been determined. The original data can be represented as the real part, real, in the following way after each IMF component has undergone the Hilbert transform:

$$X(t) = Real \sum_{j=1}^{n} aj(t).e^{i\int \omega j(t)dt} \quad (2.14)$$

2.3.3 PQDs classifying by Artificial intelligence

Artificial intelligence (AI) technologies have emerged as a strong alternative to solving problems that require human reasoning in the modern era. With a strong mathematical foundation, AI techniques emerged into effective instruments for accurately identifying PQDs. Shape similarity degrades power quality, and all of these distorted signals need to be processed fast. Therefore, AIs are required for power quality disturbance classification, and they have proven to be able to manage data obtained by detection algorithms and classify disturbances [22].

2.3.3.1 Artificial neural network

Neural network-based classification is a viable replacement when adequate data is available [26].The authors offered a powerful ANN classifier for data derived from power quality disruptions in smart grids, based on the DWT approach [26]. It was looked at how electrical signals were categorized into voltage sag, voltage swell, and interruption [28]. The synthetic power quality signals that were supplied to the DWT were generated using Matlab. The noise

was eliminated after the synthetic signals were produced using signal wave equations. The signals were routed to DWT for change point identification following filtering. Before the signals were delivered to SVM for classification, they were first segmented using the change points that DWT had discovered. However, ANN employs several activation functions and multi-layer connections to address nonlinear problems.

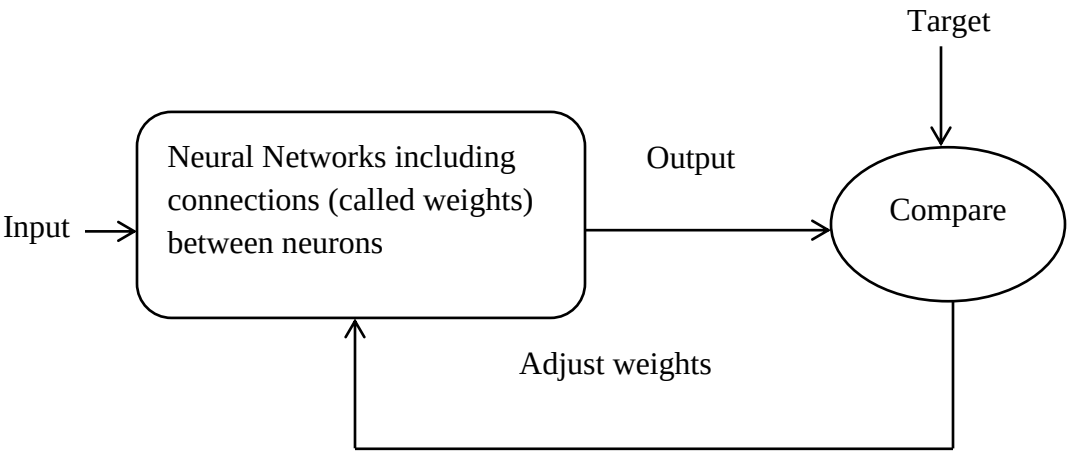

Figure 2. 3 flowchart of ANN

2.3.3.2 Support Vector Machine

Supervised learning machine algorithms, or SVMs, are used to identify patterns in a wide range of research and classification systems. Vapnik and associates first presented the support vector machine (SVM) concept (N. Vapkin, 2010) [7]. One technique for forecasting, estimating, and problem solving is pattern recognition, which is based on statistical learning theory. The crated signals were sent into the Stock well transform, which creates a ST matrix by using a second-order Gaussian window. This matrix is then used as input for the Support Vector Machine (SVM), extracting features like energy and the standard deviation of the phase contour and magnitude. No mitigation technique was used.

Computing the (soft-margin) SVM classifier amounts to minimizing an expression of the form:

$$[\ \frac{1}{n}\sum_{i=1}^{n}\max(0,1-yi(W^T Xi-b))] +\lambda \|W\|^2 \qquad (2.15)$$

Choosing a sufficiently small value for λ yields the hard-margin classifier for linearly classifiable input data.

The optimization problem as follows:

$$minimize\ \frac{1}{n}\sum_{i=1}^{n}\xi\, i + \lambda\, \|W\|^2 \qquad (2.16)$$

Subject to $yi(W^T xi - b) \geq 1 - \xi i\ \&\ \xi\, i \geq 0\ , for\ all\ i$

This is called the primal problem.

By solving for the Lagrangian dual of the above problem, one obtains the simplified problem

$$maximize\ f(c1 \ldots . cn) = \sum_{i=1}^{n} ci - \frac{1}{2}\sum_{i=1}^{n}\sum_{j=1}^{n} yici(Xi^T Xj)yjcj \qquad (2.17)$$

$$\text{Subject to } \sum_{i=1}^{n} ciyi = 0, and\ 0 \leq ci \leq \frac{1}{2n\lambda} for\ all\ i \qquad (2.18)$$

This is called the dual problem.

We know the classification vector w in the transformed space satisfies

$$W = \sum_{i=1}^{n} ciyi\varphi(xi), \qquad (2.19)$$

Where, the c_i are obtained by solving the optimization problem

$$maximize\ f(c1 \ldots . cn) = \sum_{i=1}^{n} ci - \frac{1}{2}\sum_{i=1}^{n}\sum_{j=1}^{n} yici(\varphi(xi) * \varphi(xj)))yjcj \qquad (2.20)$$

$$= \sum_{i=1}^{n} ci - \frac{1}{2}\sum_{i=1}^{n}\sum_{j=1}^{n} yicik(xi, xj)yjcj$$

$$\text{Subject to } \sum_{i=1}^{n} ciyi = 0, and\ 0 \leq ci \leq \frac{1}{2n\lambda} for\ all\ i \qquad (2.21)$$

The coefficients c_i can be solved for using quadratic programming.

2.3.3.3 Fuzzy Expert System (FES)

The fuzzy expert system (FES), one of the traditional AI methods, is based on two possibilities for decisions in ambiguous situations. The calculation that the human mind can use boundary less models serves as its motivation. The membership function, also known as the planning of objects at a given domain to their membership values, is a function of fuzzy systems.

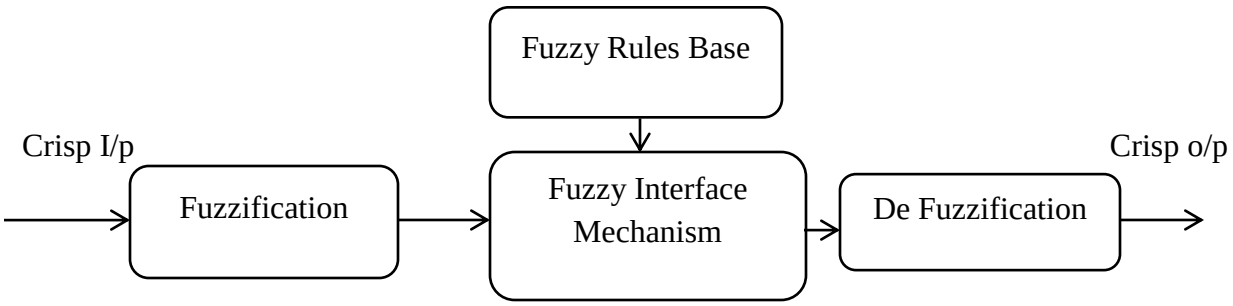

Figure 2. 4 Flowchart of fuzzy expert system

2.4 Classification of Power Quality Disturbances

2.4.1 Power quality

Voltage unbalance in three-phase systems, extended outages, system dependability, and the power electronics' interface with an electric power source are only a few of the many variables that make up power quality [35].

2.4.2 Power quality Standard's

By following Power quality standards, electrical power systems can be made more reliable overall, experience lower equipment failures, and use less energy. These guidelines must be followed by companies, manufacturers, and utilities to guarantee a reliable and effective power supply.

The criteria are used as a guide to measure and assess the electrical power supply's quality. They guarantee consistent measurements, help determine the kinds of power quality problems that occur, and guarantee that power systems fulfill particular dependability and quality requirements.

When power quality problems become severe enough to affect both issue makers and consumers, there is cause for concern. As a way to restore the level of power quality to an suitable scale and to give customers, manufacturers, and utilities standards on lowering the various events causing the power quality issues, a number of organizations, including the IEEE, IEC, computer business equipment manufacturers association (CBEMA), British standards (BS), European norms (EN) and information technology industry council (ITIC), have advanced several standards [35].

Table 2. 2 Standards of Power quality

PQ's Problem	PQ Standards
Monitoring & definition of electric power Quality	IEEE 1159
Voltage disturbance	EN 50160
Measurement of electrical quantities under different situations	IEEE 1459
Electromagnetic compatibility	IEC 61000
Power and grounding	IEEE 1100
Steady-state voltage ratings	ANSI C84.1 (For America)
Voltage disturbance	AS/NZS 61000

2.4.3 Power Qualities Disturbance (PQD)

Power Quality (PQ) is well-defined in a variety of ways in the industry, but generally speaking, it is defined as fewer interruptions, better electrical system performance, and less system malfunction from the standpoint of the customer. PQ, as viewed by the utility, is the dependability of the power supply that generators provide to customers. The consistency of voltage or current in an electrical system exhibiting a sinusoidal characteristic is another way to describe PQ; deviations from this definition indicate lower PQ. PQ concerns are defined as any changes in magnitude or frequency of current or voltage that effect system performance and consumer equipment. Both utilities and customers may suffer greatly as a result of these aberrations. PQ phenomena can be divided into steady-state and non-steady-state categories, each of which is distinguished by particular traits.

2.4.3.1 Voltage Sag

The decrease in the standard rms voltage from 0.1 pu to 0.9 pu is known as voltage sag. It is usually produced by a Single Line to Ground (SLG) fault, motor starting, or the presence of overcurrent, and it can last anywhere from 0.5 cycles to 1 minute. A momentary dip in voltage is also referred to as voltage sag, whereas a decrease in voltage lasting more than one minute is

classified as under voltage. Based on duration, voltage sag can be divided into three classes: immediate, momentary, and temporary. A transformer fault or other breakdown in the utility power system may cause voltage sag.

2.4.3.1 Voltage Swell

When the RMS voltage rises between 1.1 and 1.8 pu at frequency lower than voltage sag, this is known as voltage swell. Similar to voltage sag, voltage swell usually lasts between 0.5 cycles and 1 minute. Various circumstances can produce voltage swells, including starting large motors, SLG faults, light system loading, and erroneous tap settings of transformers. There are three types of SLG fault-induced swelling: immediate, momentary, and temporary. It happens throughout unfiled phases. Overvoltage occurs when the elevated voltage lasts longer than one minute. Installing tap changers with quick action can assist in reducing voltage swell. Increased iron loss in machinery applications and overheating of DC regulators are two effects of voltage swell.

2.4.4 Dynamic Voltage restorer (DVR)

Distribution systems can now compensate for voltage-related power quality problems because of developments in custom power device technology. Dynamic Voltage Restorers (DVRs) may eliminate a variety of voltage disturbances, including spikes, sags, swells, notches, and harmonics, as well as effectively resolve voltage imbalances in three-phase systems, control terminal voltage, and lessen flicker [35]. DVRs add a voltage component in line with the source voltage to offset load-side voltage variations. In the event of unpredictable network conditions, a rapid control reaction assures a stable voltage supply within about 3 milliseconds. The ability to actively transmit power is illustrated through the injection of an arbitrary phase of voltage for the load current. This active power is transferred over the DC connection and can originate from an energy storage device, a diode bridge connected to the AC network, or a shunt-connected PWM converter. DVRs are essential for preserving a steady and reliable power supply because they balance voltages, control voltage levels, and stop source voltage harmonics from influencing the load.

2.4.4.1 DVR Working and Control Principle

DVR is an IGBT based VSC (Voltage Source Converter) with a DC bus capacitor that employs a control algorithm to predict and regulate injected voltages. In situations where indirect voltage

control is necessary, reference load voltages can be calculated instead of injected voltages. Hysteresis (carrier-less PWM) or PWM (fixed-frequency) voltage control is utilized to generate gate pulses for the DVR. The primary function of DVRs is to safeguard sensitive customer loads from various disruptions such as voltage imbalance, sags, swells, and waveform distortion. By injecting voltages (Vinj) in series with the source, DVRs ensure that the load voltage remains constant and free from distortion even in cases where the supply voltage is not stable or may be distorted.

The key components of a dynamic voltage restorer (DVR) include:-

I. Injection (Booster) Transformer

Using HV windings, an injection (booster) transformer links the DVR to the distribution network. It isolates the load from the system and couples the compensatory voltages generated by the voltage source converters to the incoming supply voltage.

II. Voltage Source Converter (VSC)

A VSC is a power electronic system that can produce a sinusoidal voltage at any desired frequency, magnitude, and phase angle. It is made up of switching and storing components. The VSC is utilized in the DVR application to either create the missing portion of the supply voltage or temporarily replace it. Metal Oxide Semiconductor Field Effect Transistors (MOSFET), Gate Turn-Off Thyristors (GTO), Insulated Gate Bipolar Transistors (IGBT), and Integrated Gate Commutated Thyristors (IGCT) are the four primary switching device types utilized in VSC. Because of its high switching frequency (short switching times) and minimal ON state power loss, IGBT is utilized in this situation as a switching device to compensate for voltage sags and swells.

III. Energy Storage

Storage devices are used to provide the VSC with the energy it needs to generate injected voltage through a DC link. Batteries, capacitance, and superconductive magnetic energy storage are the various types of energy storage devices.

IV. Control unit

Monitors the voltage levels and commands the VSI to inject or absorb power as needed to maintain voltage stability.

V. Filter unit

Serve to smooth out any harmonics or distortions in the output voltage to ensure a spotless and stable power supply.

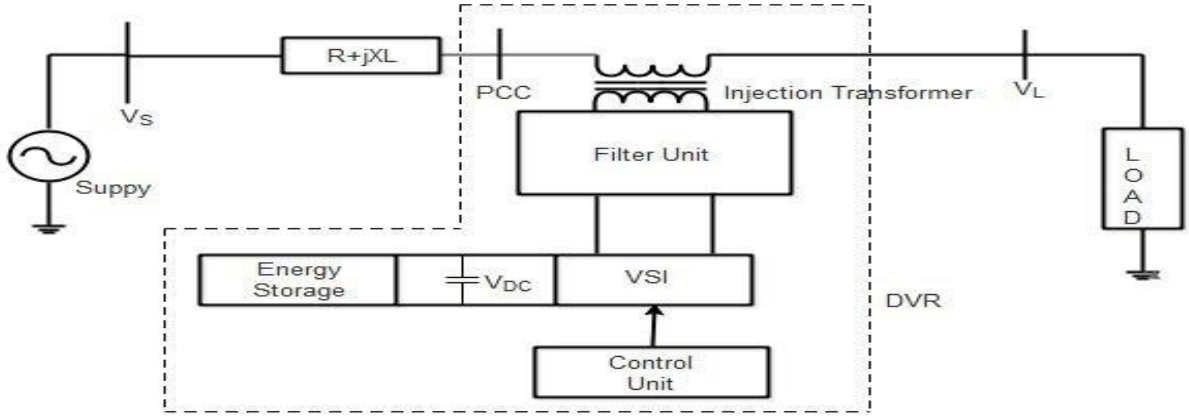

Figure 2. 5 schematic diagram of DVR

Chapter Three

Materials and Methods

3.1 Introduction

Hawassa distribution has 15KV line system with two Transformer feeders I and Transformer feeders II and two transformers with 2x25MVA rating works with parallel for Hawassa distribution substation. Those two Feeders are supply 15KV to the consumers through eight feeds such as Feeder 1, Feeder 3, Feeder 4, Feeder 5, Feeder 6, Feeder 7, Feeder 8, and Feeder 12. Feeder 6 (R4-G5) is covered in this thesis. Data was acquired from secondary sources, from Ethiopian Electric Utilities (EEU) Hawassa No. 3 customer service center network infrastructure management office current recorded data. Voltage, current, and power measurement records acquired with a 15 KV SCADA management system were among the data from Ethiopian Electric Utility. The Hawassa electric power distribution network's 15 KV substation one (SS1) has comprehensive information on how it is connected to feeders, transformers, and switching stations.

Serving a sizable customer base in the Hawassa area, the Hawassa Substation of Feeder Six is an essential electrical distribution point. This feeder, which has an 8.76 megawatt capacity, is important to providing a steady source of electricity to the region's numerous residential, commercial, and industrial customers. A wide variety of consumers, including homes, companies, educational institutions, hospitals, and manufacturing facilities, are included in the customer statistics for Feeder Six's Hawassa Substation.

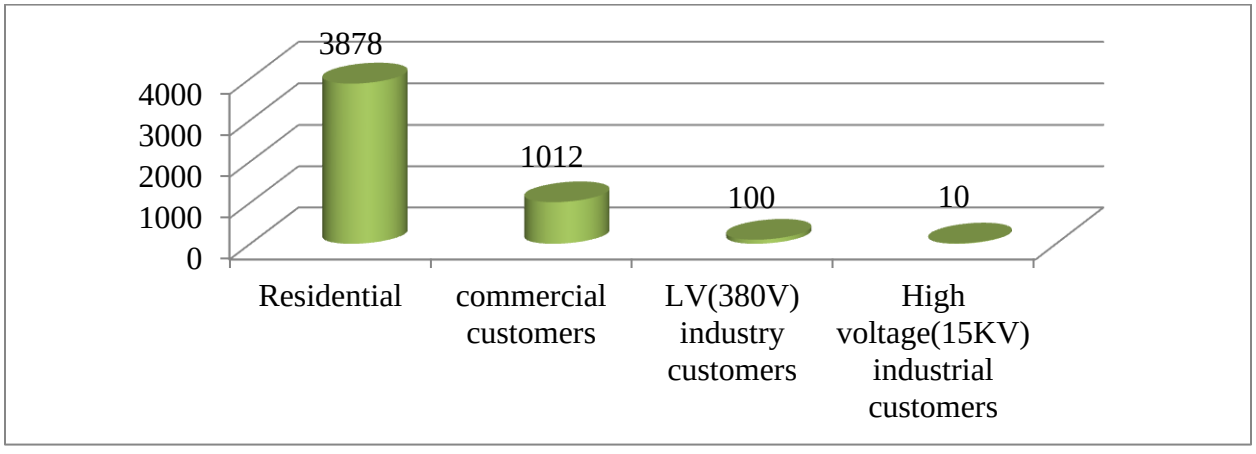

Figure 3. 1 Total customer of Hawassa distribution network feeder six (R4-G5).

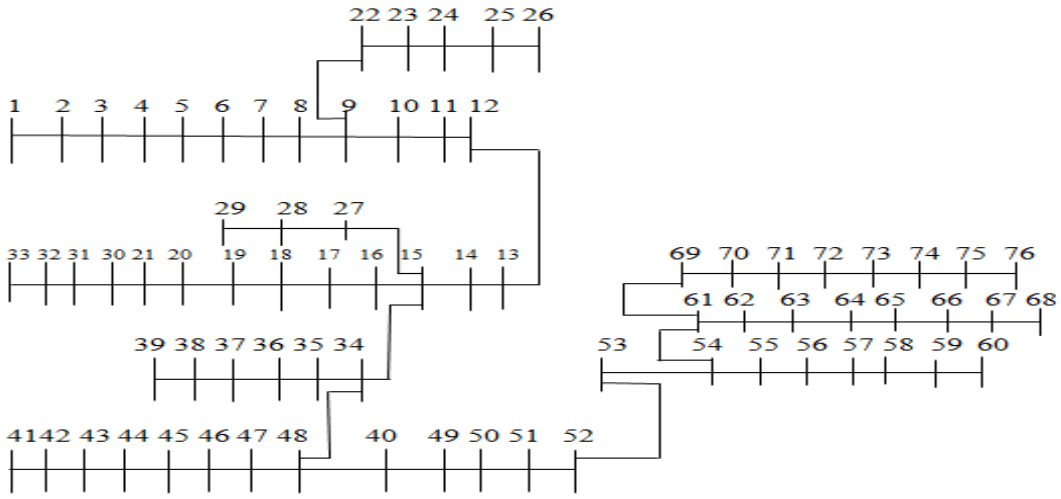

Figure 3. 2 Single Line Diagram of R4-G5

3.2 Data gathering of hawassa distribution network

The information needed for this thesis was obtained from EEU (Sidama Electric Utility Hawassa No.3 customer service center network infrastructure management office) during the Hawassa distribution network survey. The information needed includes the feeder's length, the transformer's rating and quantity, and the load of each transformer, all of the historical data was recorded in recent months in detail.

Table 3. 1 Hawassa distribution network feeder six (R4-G5) transformer rating and type

No	Feeder name	Transformer Rating(KVA)	Quantity
1	Feeder 6(R4-G5)	25	4
2		50	11
3		100	20
4		200	19
5		315	17
6		400	1
7		500	2
8		630	2
		Total = **76**	

Table 3. 2 Distance Coverage of the Feeder

Distance point	Distance (km)
From old substation to RMU(doro erebata)	7
From RMU(R4-G5) to End	80

Table 3. 3 Incoming and outgoing Hawassa substation one

Transformer capacity	Feeder line	Rated Voltage(15KV)	Yearly average load (MW)	Feeder CT Ratio
132KV/15KV/2*25MVA	Feeder 1	15	4.4	400/1
	Feeder 3	15	6.4	400/1
	Feeder 4	15	6.3	400/1
	Feeder 5	15	6.2	400/1
	Feeder 6	15	8.76	400/1
	Feeder 7	15	1.1	400/1
	Feeder 8	15	3.24	400/1
	Feeder12	15	4.47	400/1
132KV/33KV/16MVA	Feeder 9	33	0.59	150/1
	Feeder 10	33	0.46	150/1
	Feeder 11	33	1.02	150/1

3.3 Power flow analysis

An essential technique in electrical engineering for examining the steady-state functioning of electrical power systems is power flow analysis. It entails resolving a series of equations that depict the system's power balance while accounting for different elements like loads, transmission lines, transformers, and generators. Power flow analysis's primary objective is to

ascertain the actual and reactive power flows on the distribution lines, as well as the voltage magnitude and phase angle at each bus (node) in the system. For the electricity system to operate steadily, dependably, and effectively, this information is essential.

The Newton-Raphson approach, the Gauss-Seidel method, and the rapid decoupling method are some of the techniques used to solve power flow equations. To arrive at a solution that satisfies the power flow equations, these approaches rely on iterative numerical techniques.

3.4 System Modeling

Hawassa feeder-6 (R4-G5) consists of 76 branches. Total active and reactive power losses of before dvr 1913.3kw and 1202.4Kvar, respectively. The single-line diagram of the system before DVR and its loops is shown in figure 3.3 and 3.4.

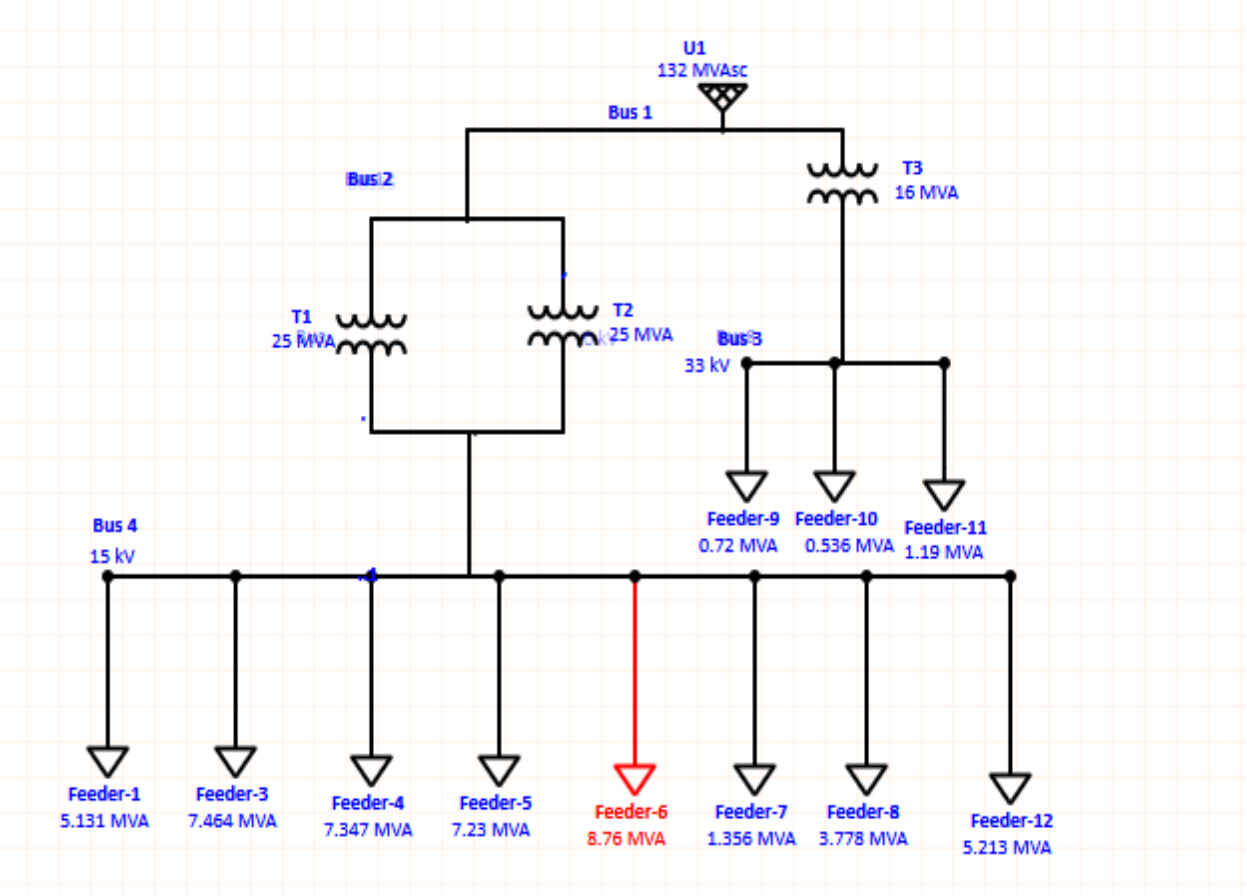

Figure 3. 3 single line diagram of hawassa substation

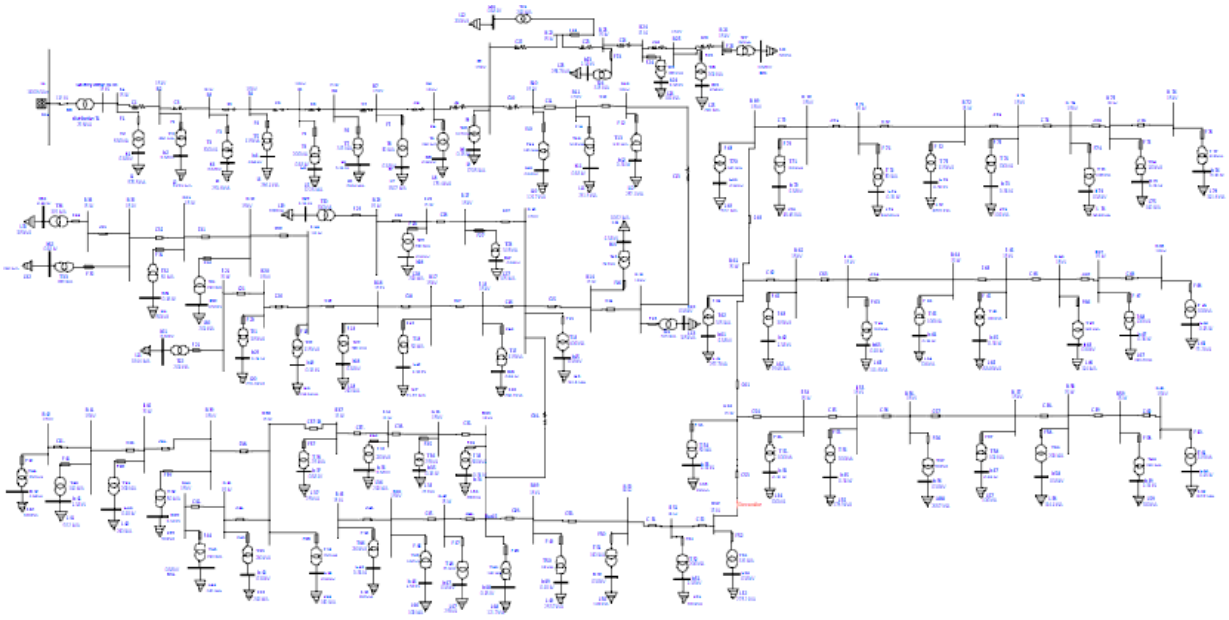

Figure 3. 4 single line diagram of Feeder 6(R4-G5) 76 Bus.

3.5 Flowchart of Wavelet transforms

To detect, categorize, and address power quality issues, it is crucial to routinely examine the voltage and current waveforms at the rated of power frequency. In order to transform the data from the voltage or current signals into useful information, key features are extracted and processed. For example, features that aid in the detection of power outages can be extracted by normalizing the input waveform. In order to simulate actual power quality problems, both single and multiple waveform patterns for different disturbances are produced during the detecting step. Using model equations, several samples are generated for every disturbance in the Matlab workspace environment.

Signal specification and setting: - is used to describe how the electrical signals that will be measured and examined will be defined in terms of their parameters and properties. This entails defining the measuring range, the sampling rate, the signal type (such as voltage, current, or power), and the necessary precision.

Modeling of Power Quality Disturbance Events: - the fundamental reasons for disruptions, such as malfunctions, switching processes or changes in load.

Detection based on discrete wavelet transform (DWT):- is an effective instrument for examining signals at various scales. It is especially well-suited for identifying important features

in power quality data because of its capacity to break down signals into details and approximations at different resolution levels. Relevant signal characteristics, including frequency, amplitude, and duration, can be extracted using DWT and utilized for categorization or additional analysis.

Decomposition of Power Quality Disturbances (PQDEs) and Feature Extraction: - Multi-Resolution Analysis (MRA) is a potent method for breaking down signals into several resolutions or scales. It is especially helpful for studying power quality disturbances (PQDEs) because it can record both the signal's voltage sag and swell components.

Feature Extraction: - Several properties, including energy, mean, min, and max, can be retrieved from the approximation and detail coefficients after the signal have been decomposed.

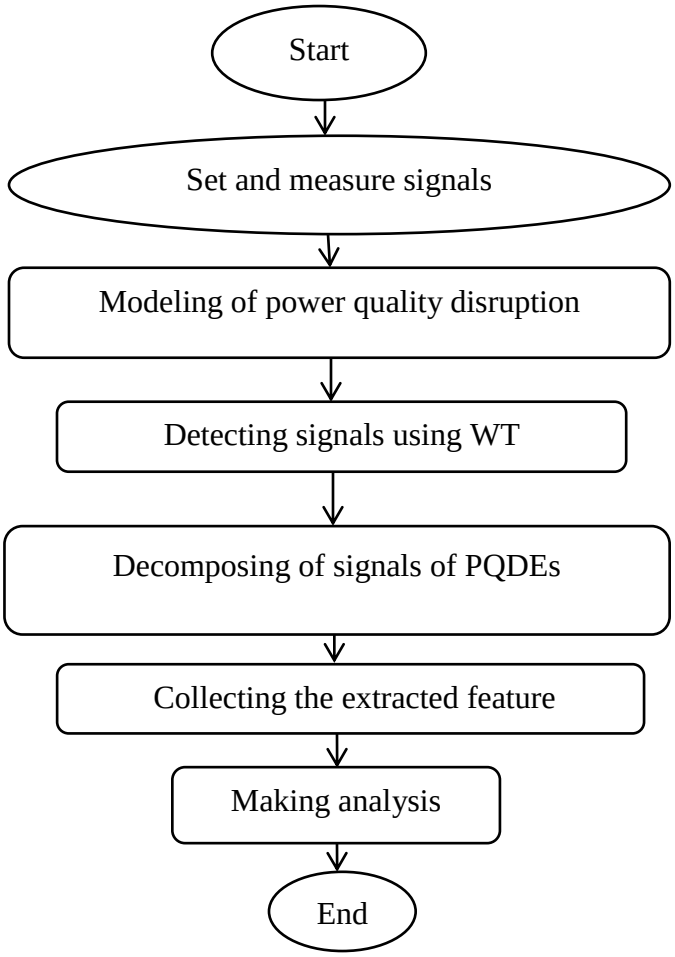

Figure 3. 5 flow chart of Wavelet Transforms.

3.6 Wavelet transform integrated with Simulink

MATLAB is used to construct simulation and modeling tools by merging wavelet transformations with Simulink. The integration makes it possible to process data and signals in real time, which makes it possible to identify errors as soon as they happen. In Simulink, wavelet transform can be combined with DVR (Dynamic Voltage Restorer) to mitigate voltage sag and swell brought on by power system problems. In signal processing, the wavelet transform can be used to detect various power system problems.

Steps to follow:

1. Design the power system model: To begin, import the Simulink model of the power system. Loads and the DVR should be included. Configure the model of the power system with the proper ratings, impedance values, and fault locations.

2. Apply different types of faults: Make many fault situations in the model of the power system. Voltage sags or swells can be caused by short circuits, line failures, or abrupt changes in load. When a disturbance is detected, activate the DVR using the wavelet transform block's output. In order to reduce sag or swell and keep the voltage quality within allowable bounds, the DVR can then inject the proper compensation voltage.

3. Implement the DVR control algorithm: Create a Simulink control algorithm for the DVR. This algorithm should determine the necessary compensation, identify any voltage sag or swell, and regulate the DVR to inject or absorb the proper amount of reactive and actual power.

4. Simulate the system: Run Simulink simulations to see how the power system reacts to various fault scenarios both with and without the DVR. Examine the voltage profile at various points across the system to determine how well the DVR reduces voltage sag and swell.

5. Optimize the DVR performance: Adjust the parameters of the control algorithm to improve the DVR's ability to mitigate voltage sag and swell. To make sure the DVR maintains system stability and offers sufficient voltage support test the system under a variety of fault scenarios.

6. Analysis the result: Compare the voltage profiles in the simulation with and without the DVR to confirm how well it mitigates voltage disruptions.

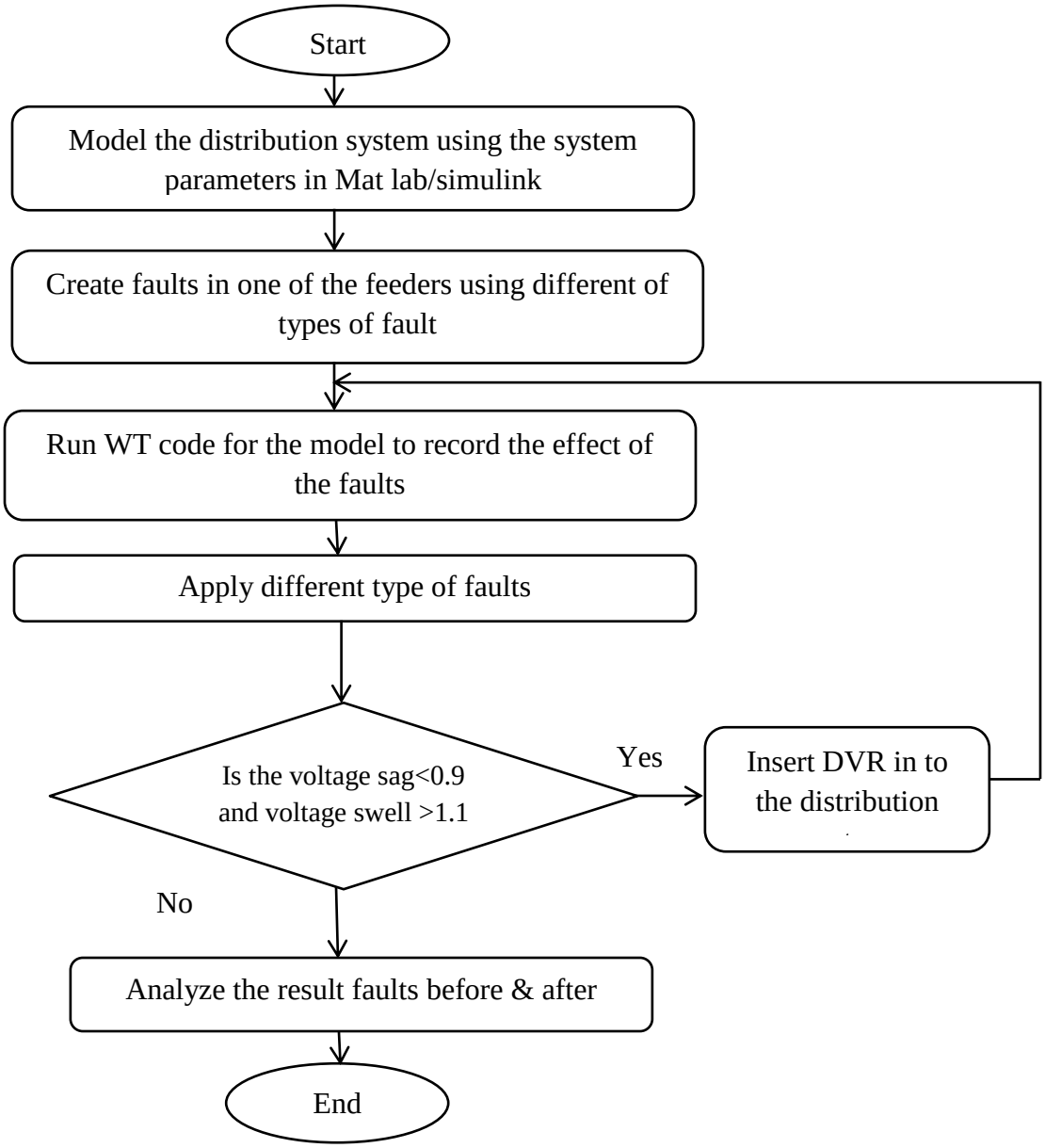

Figure 3. 6 flow chart of a wavelet transform integrated with Simulink.

3.7 Overall system modeling

For ETAP software to accurately model and simulate power systems and analyze variables like power flow, voltage stability, system losses, and equipment sizing, input parameters (transformer KVA, length of feeder, and load) are necessary. To define the values of resistance (R), reactance (X), real power (P), and reactive power (Q) at different places in the power system, simulations would be done as part of the load flow study.

The findings of the load flow analysis can be used to determine the desired output values of resistance, reactance, real power, and reactive power. Next, one can enhance the Grasshopper optimization algorithm's performance and guarantee that it converges to an ideal solution quickly by properly configuring the input data parameters.

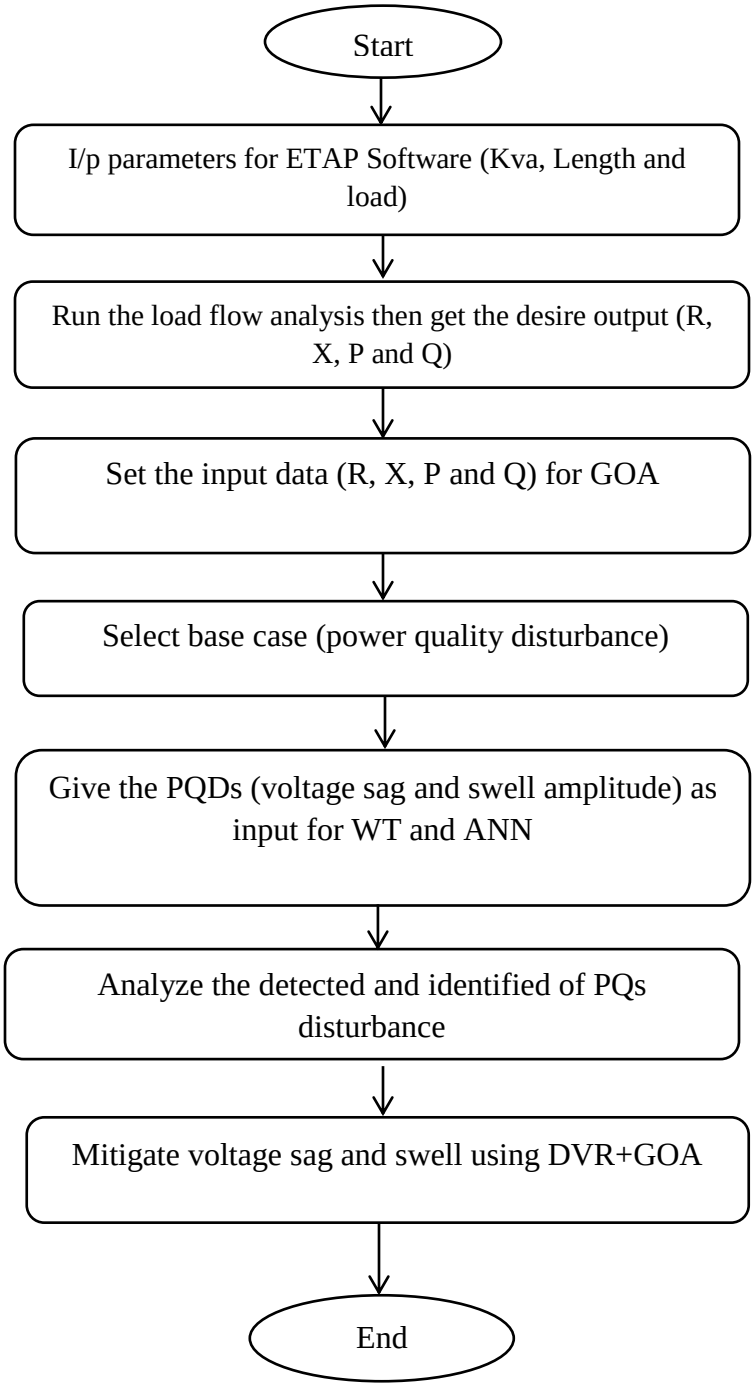

Figure 3. 7 General Block Diagram of power quality disturbance

3.8 Power flow in the feeder

The network experiences two different kinds of power loss: reactive power loss, which is brought on by reactive components, and active power loss, which is brought on by the lines' resistance. Because it lowers the efficiency of energy transmission to customers, active power loss is a big worry for utility providers. To guarantee voltage stability, it's also critical to keep the system's reactive power flow at an appropriate level. The initial active power loss in the Hawassa distribution system was 1913.3 kW, while the reactive power loss was 1202.4 kVAR. At bus 76, the system's minimum voltage was 0.714538471 pu.

3.8.1 Backward/Forward Sweep Based Distribution Load Flow Method

The backward/forward sweep based distribution load flow method is a numerical technique used to analyze power distribution systems. In this thesis, the algorithm iteratively calculates the voltages and power flows at each bus in the distribution network. The process involves two separate sweeps: a backward sweep and a forward sweep.

During the backward sweep, the algorithm starts at the substation or primary feeder and works its way towards the loads. It calculates the voltages and power flows at each bus based on the known values at neighboring buses and the line parameters.

Backward sweep: At iteration k, starting from the branches in the last layer and moving towards the branches connected to the root node, the current in branch L, JL is calculated as

$$JL(K) = -IL2(K)\sum(Currents\ in\ branches\ \ emnating\ from\ node\ L2)\ \mathrm{L} = \ \mathrm{b}, \mathrm{b} - 1, \ldots \ldots \ldots \quad (3.1)$$

Where IL2(k) is the current injection at node L2. This is the direct application of the KCL.

Once the backward sweep is completed, the algorithm then performs a forward sweep starting at the loads and working its way back towards the substation. This process adjusts the voltage levels at each bus to account for the power losses and ensure the overall system remains balanced**.** By iteratively running the backward and forward sweeps until convergence is reached, the algorithm can determine the steady-state operating conditions of the distribution system, such as voltage levels, power flows, and line losses.

Forward sweep: Nodal voltages are updated in a forward sweep starting from branches in the first layer toward those in the last. For each branch, L, the voltage at node L2 is calculated using

the updated voltage at node L1 and the branch current calculated in the preceding backward sweep.

$$VL2^{(K)} = VL1^{(K)} - ZLJL^{(K)}\ L = 1,2,\dots\dots,b \quad \text{(3.2)}$$

Where, ZL is the series impedance of branch L. This is the direct application of the KVL

3.9 Optimization approach to enhance the voltage level

3.9.1 Grasshopper optimization Algorithm

Due to their potential to harm crops, farmers view grasshoppers as pests. In quest of food, grasshoppers move randomly when they are by themselves, but in a swarm, they move in unison, resembling rolling cylinders. These swarms are dangerous to agricultural areas because they can eat nearly any crop that gets in their way. Attraction and reproduction forces force the grasshoppers in the swarm to keep a comfortable distance from one another. The fact that grasshoppers are either drawn to one another when they are too far apart or repulsed when they are too close together serves as an example of this dynamic.

The mathematical modeling of grasshopper swarming behavior is described in the following way.

$$P_i = S_i + G_i + A_i \quad \text{(3.3)}$$

Where P_i indicates the i grasshopper 'position, S_i is the social interaction between grasshoppers, G_i denotes the gravity force on the i grasshopper, and A_i is the wind advection. To harvest a random behavior of grasshoppers, Equation (3.8) can be rewritten as follow.

$$P_i = r_1 S_i + r_2 G_i + r_3 A_i \quad \text{(3.4)}$$

Where r_1, r_2 and r_3 is random numbers in the range [0, 1]

The social interaction $S_i$is defined as follows:

$$si = \sum_{j\neq i, i=1}^{N} S(dij)dij \quad \text{(3.5)}$$

Where N means the number of grasshoppers, d_{ij} $|pj - pi|$ defines the Euclidean distance between the i^{th} grasshoppers and dij $= \frac{pj-pi}{dij}$ is a unit vector from the i^{th} grasshopper to the j^{th} grasshopper, and s represents the social forces designed by the following equation:

$$s(r) = f exp^{\frac{-r}{l}} - exp^{-r} \quad \text{(3.6)}$$

Where, f and l stand for the scales of attraction length and intensity, respectively. Attraction and repulsion are two ways that grasshoppers interact socially. The range [0, 15] takes the distance into account. The attraction gradually diminishes after increasing between [2.079, 4]. The range in which the repulsion takes place is [0, 2.079]. There is neither attraction nor repulsion (no force) when two grasshoppers are precisely 2.079 apart. We refer to this space as the comfort zone.

The gravity force G_i is given by the following equation:

$$G_i = -ge_g \tag{3.7}$$

Where g denotes the gravitational constant and e_g denotes a unit vector toward the center of earth. The wind advection A_i is given by the following equation:

$$A_i = ue_w \tag{3.8}$$

Where u denotes the drift constant and e_w is a unit vector in the wind direction. After replacing the values of S; G; and A, the following equation can be obtained.

$$p_i = \sum_{j\neq i, i=1}^{N} s(|p_j - p_i|)\frac{p_j - p_i}{dji} - ge_g + ue_w \tag{3.9}$$

Equation (3.14) cannot be used straight to solve optimization problems, as the grasshoppers reach fast the comfort zone and the swarm system does not converge to a target location. An enhanced version of this equation is given as:

$$p_i = c\left(\sum_{j\neq i, i=1}^{N} C\,\frac{U_{bd} - I_{bd}}{2}\, s\left(\left|p_j^d - p_i^d\right|\right)\frac{p_j - p_i}{d_{ji}} + T_d\right) \tag{3.10}$$

Where U_{bd} and I_{bd} represent the upper and lower bounds in the d^{th} dimension, respectively. T_d represents the best solution found so far in the d^{th} dimension space.

The parameter C_2 is used to decrease the repulsion zone, attraction zone, and comfort zone between grasshoppers similarly to the number of iterations. C_1 and C_2 are considered as a single parameter and it is expressed using the following equation.

$$C = C_{max} - t\frac{C_{max} - C_{min}}{t_{max}} \tag{3.11}$$

Where C_{max} and C_{min} denote the max and min values of C respectively, t is the current iteration and is the maximum number of iterations. The position of a grasshopper is updated based on its

current position, global best position, and the positions of other grasshoppers within the swarm. This helps GOA to avoid getting trapped in local optima.

3.10 Problem formulation

Problem Formulation for Bus Voltage Profile Improvement Using Grasshopper Optimization Algorithm (GOA)

1. Objective Function

The main objective is to compensate voltage limit violations while minimizing voltage variances from the nominal value (1.0 per unit) across all busses.

The objective function is formulated as follow:-

$$f = \sum_{i=1}^{N}(V_i - V_{ref})2 + \lambda \sum_{i=1}^{N}[\max(0, V_i - V_{max}) + \max(0, V_{min} - V_{i)}] \quad (3.12)$$

Where:

- v_i= Voltage magnitude at bus i,
- v_{ref} = 1.0 pu.,
- V_{min}, V_{max}= Voltage limits (e.g., 0.95–1.05 p.u.),
- λ= Penalty factor for constraint violations.

The following formula defines the current flow through the line:

$$In_{o,n+1} = \frac{v_{no,n+1} < \delta_{no,n+1} = v_{no,n+1} < \delta_{no,n+1}}{R_{no,n+1} + jx_{no,n+1}} \quad (3.13)$$

The branch's reactance is X_{n+1}, and its resistance is R_{n+1} .The power consumed by the loads is as Follows:

$$p_{n+1} - jQ_{n+1} = V_{n+1} * I_{n+1} \quad (3.14)$$

The general active and reactive Power loss is denoted by p_{n+1} and Q_{n+1}, respectively as follows:-

$$P_{n+1} = \sum_{j=n+1}^{N} P_{L,j} + \sum_{j=n+1}^{N} P_{loss,j} \quad (3.15)$$

$$Q_{n+1} = \sum_{j=n+1}^{N} Q_{L,j} + \sum_{j=n+1}^{N} Q_{loss,j} \quad (3.16)$$

There are N buses in entire in this case. On the bus j, both active as well as reactive loads are $P_{L,j}$ together with $Q_{L,j}$ respectively. Over the branch, the active power is lost is denoted by $P_{loss,j}$ and the reactive power loss by $Q_{loss,j.}$

$$P_{loss,n} = \frac{R_n(P^2n+Q^2n)}{|V_n|^2} \quad (3.17)$$

$$Q_{loss,n} = \frac{X_n(P^2n+Q^2n)}{|V_n|^2} \quad (3.18)$$

The over-all system active power loss can be determined by combining all line power losses.

$PL_{n+1} + j\ QL_{n+1}$ (3.19)

The total the branching was represented by Nb, and the feeder's topological position is represented by the binary variable Kn. One can identify the optimization problem as follows:

Minimize F = minimize (PT_{loss})

Starting from the root bus, the node voltages are updated using the following equation.

$$V_i^k = V_{i=1}^k Z_i J_i^k \ , i = 2,3 \dots \dots \dots n \quad (3.20)$$

Where Z_i is the series impedance of branch *"i-1, i.*

Those three steps are repeated until voltage magnitudes at each node in the present iteration and the previous iteration is lower than a tolerance limit ε

$$MAX\ ([V^{K+1}]-[V^{k}]) < \varepsilon \quad (3.21)$$

Subject to:-

1. Voltage Limits constraints: $V_{min} \leq V_i \leq V_{max}$

2. Device rating constraints: $C_i = \sqrt{3}V_{DVR} * I_{load}$, where C_i= is the rating of the DVR

3. Cost constraints: Minimize $C = minimum\ (PT,loss)$

4. The rules of Kirchhoff law (voltage as well as current) are as follows:

$$g_i(I,K) = 0 \quad (3.22)$$

$$g_v(V,K) = 0 \quad (3.23)$$

3.11 Mathematical Modeling of GOA (Grasshopper optimization algorithm)

Because of the harm they cause to crops, farmers view grasshoppers as harmful insects. When a grasshopper is alone in the wild, its movements are haphazard. However, it follows a coordinated path as a member of the collective after it joins a group of grasshoppers. In agricultural regions, swarming grasshoppers forage on crops as they go, moving in a systematic fashion. Through mating rituals and attraction force, the grasshoppers in the swarm are forced to maintain a specific distance from one another. When the grasshoppers are too close to one another, a repulsion force is created; when they are farther away or at a safe distance, a pulling force is created. The grasshoppers are the search agents, and the meal supply is the best place for the grasshoppers to be found in the flock. The suggested algorithm can be described in terms of the following stages:

Step 1: Stay inside the specified bounds of the control variables while you generate the starting values for the grasshopper positions at random. The number of grasshoppers (search agents) and the control variables (social interaction strength(c), wind advection strength (u) and the gravity constant) are represented by the variables w and j, respectively.

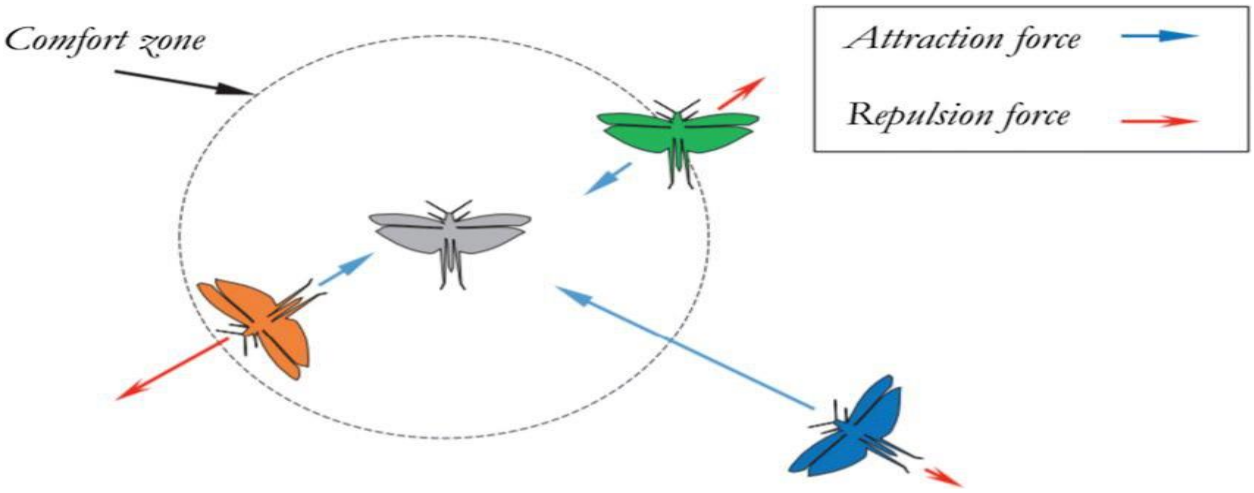

Figure 3. 8 swarm of grasshoppers in primitive corrective patterns between individuals.

Step 2: The branches that can be changed to change the systems are symbolized by the grasshopper positions created, which are stated as follows:

$$\begin{bmatrix} GS_{11} & GS_{12} \dots\dots\dots GS_{1j} \\ GS_{21} & GS_{22} \dots\dots\dots GS_{2j} \\ GS_{W1} \dots\dots\dots\dots\dots\dots\dots GS_{WJ} \end{bmatrix} \quad (3.24)$$

Step 3: Define each position's objective using the following formula:

$$\mathrm{OG} = [OG_1 OG_2 OG_3 \dots\dots OG_W]^2 \quad (3.25)$$

Step 4: starting from the top fitness score to the lowest fitness value, arrange the grasshopper in the manner indicated by:

$$GS = \begin{bmatrix} GS_{1,1,best} & GS_{1,2,best} & GS_{1,j,best} \\ GS_{w,1,worst} & GS_{n,2,worst} & GS_{w,j,worst} \end{bmatrix} \quad (3.26)$$

Step 5: updated each grasshopper's position

$$GS_i^d(a+1) = c(\sum_{j\neq i, i=1}^{w} C \ \frac{U_{pd} - L_{pd}}{2} \ s\left(\left|GS_j^d(a) - (a)\right|\right) \frac{GS_{j(a)} - GS_{i(a)}}{d_{ji}} + I_d \quad (3.27)$$

$$s(d_{ji}) = f e^{\frac{-d_{ji}}{l}} - e^{-d_{ji}} \quad (3.28)$$

$$C = C_{max} - a \frac{C_{max} - C_{min}}{a_{max}} \quad (3.29)$$

The variables a, a_{max} , C_{max} ,and C_{min} indicate the current iteration, max and min values in relative to factor c, respectively, and add up to one, 1, and 0.00001, Where The range of capturing lengths is symbolized by l, while the level of attraction is denoted by f. The separation of the grasshoppers I and j is d_{ji} . Id: is an ideal placement attained thus far GS_i^d. The d-th dimension's i-th grasshopper is denoted by the letter id (I = 1, 2, w) within the swarm of grasshoppers, there are social forces of attraction as well as repulsion are defined by the function.

Step 6: step 3 through step 5 should be repeated till the highest possible quantity of current iteration is reached.

Step 7: After the setup is done, show the desired position that signifies the best outcome by placing the dvr and finding the desired level of efficiency with minimal power loss.

Step 8: print out the fitness objective, which represents the minimum level of power system loss, improved voltage level and the preferred location for dvr.

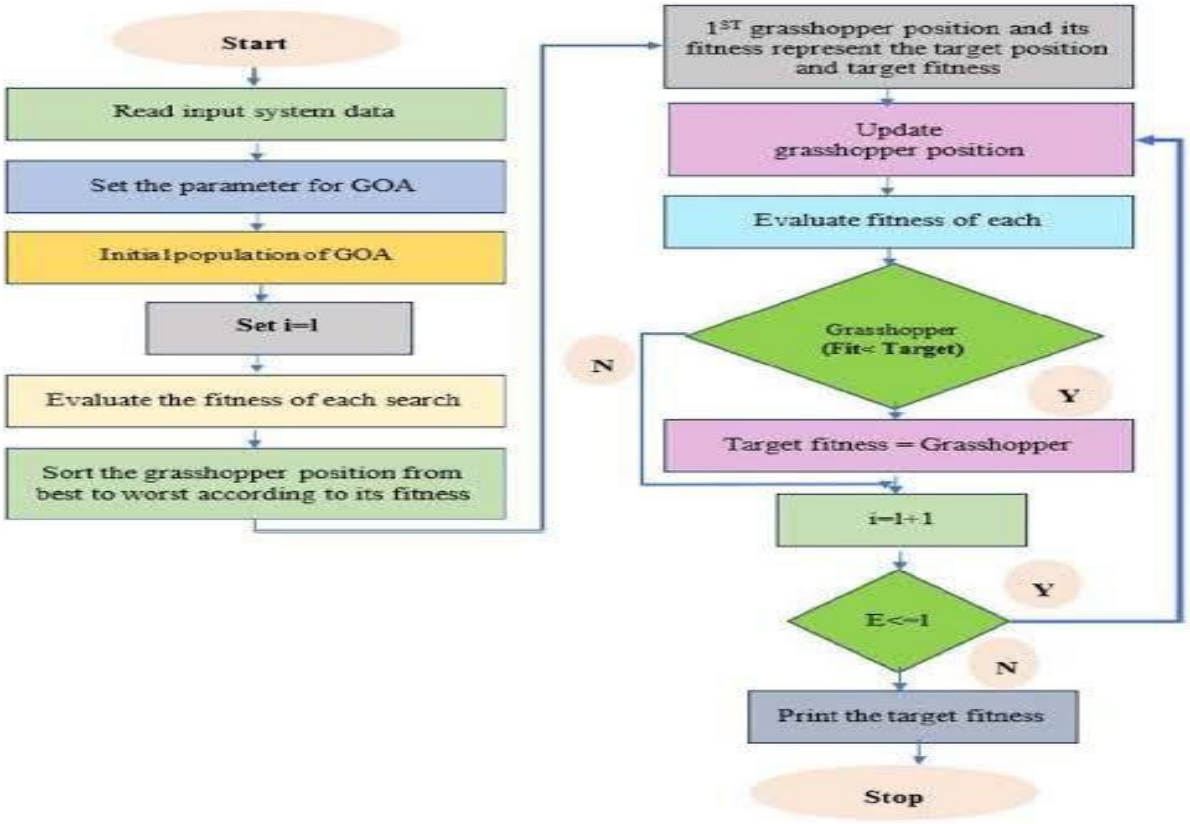

Figure 3. 9 Flowchart of grasshopper optimization algorithms.

3.12 Design of Mitigation Mechanism for Power Quality Disturbance

3.12.1 Design of Dynamic voltage restorer (DVR)

Feeder 6 is the feeder highly adversely affected of the nine feeders. When choosing (feeder 6), there are two outgoing feeders with a total active and reactive power of 8.76 MW and 2.72 MVAR, respectively.

During normal condition

Calculating the apparent power, $S = \sqrt{(P^2 + Q^2)}$ (3.30)

Where P = Average active power of the bus = 112.54 KW and Q = Average reactive power of the bus = 65.856KVAR.

$$S = \sqrt{112.54^2 + 65.85^2} = 130.4\text{kva}$$

Power factor, $cos\phi = \frac{Active\ power}{Apparent\ power}$ (3.31)

$\cos\phi = \frac{P}{s} = \frac{112.54KW}{130.4KVA} = 0.86$, $\sin\phi = \sqrt{1-(\cos\phi)^2} = 0.51$, and $\phi = \cos^{-1}(0.86) = 30.68^{o}$

Assume that the supply frequency is 50Hz, the three-phase supply line voltage is fs=380V, the load is 380V, the apparent power (S) is 130.4KVA, and the lagging power factor is 0.9. The DVR is mounted on the load-connected side of the transformer, which has a delta star connection to step 15kV down to 380V. In order to achieve unity power factor at the AC mains without voltage sag, the same power angle must be maintained for equal reactive power sharing in both VSCs under steady-state conditions.

The minimum tolerance is ±10% voltage deviation (sag or swell) of source with base value of 380V.

Phase load current, $I_{LP} = Apparent\ Power / 3*phase\ load\ voltag$

The three phase supply phase voltage, $VSp = Line\ Voltage/\sqrt{3}$ (3.32)

$$VSp = Line\ Voltage\ /\sqrt{3} = 380V\ /\sqrt{3} = 220V.$$

Three phase load phase voltage, $VLp = Load\ Voltage/\sqrt{3} = 380V/\sqrt{3} = 220V$.

The supply current before any voltage variation is, the DVR current,

$$I_S = I_{DVR} = Load\ Active\ Power / 3*VSp \quad (3.33)$$

$$I_S = I_{DVR} = 112.54\text{kw}/3*220 = 170.51\ \text{A}$$

The reactive power rating of DVR is equal to the reactive power of the load.

$$Q_{DVR} = Load\ Reactive\ Power \quad (3.34)$$

$$Q_{DVR} = 65.85\ \text{kvar}$$

From the relation of reactive power of the DVR, the power angle is computed as follows:

The reactive power of DVR $QDVR = 3V_{LP}\ I_{SP}\ sin\ \delta$ (3.35)

$$\delta = \text{Sin}^{-1}\ (Q_{DVR}\ /3V_{LP}\ I_{SP})$$

$$\delta = \text{Sin}^{-1}\ (65.85\ \text{kvar}/3*220*170.51)$$

$$\delta = \text{Sin}^{-1}\ (0.585) = 35.80^{0}$$

The active power of DVR: $P_{DVR} = 3\ V_{Lp}\ I_{sp}\ (1 - cos\ \delta)$ (3.36)

$$P_{DVR} = 3*220*170.51\text{A}\ (1-\cos 35.80^{0}) = 21.26223\text{kw}$$

The KVA rating of DVR is $S_{DVR} = \sqrt{P_{DVR}^2 + Q_{DVR}^2}$

$$S_{DVR} = \sqrt{21.26223^2 + 65.85^2} = 69.19\text{kva}$$

The voltage rating of the DVR is $V_{DVR} = S_{DVR}/3I_{DVR}$ = 69.19kva/3*170.51 = 135.26 v

Voltage sag compensation by DVR:-

Afterward voltage sag, the source sag line voltage reduces to: $V_{Slsag} = 380(1 - 0.1) = 266\text{v}$

The supply sag phase voltage, $V_{SP\ Sag} = V_{Slsag}/\sqrt{3} = 266\text{v}/\sqrt{3} = 153.57$ v

The supply current during voltage sag compensation is,

$$Isag = \frac{Active\ power}{3 * Vspsag} = \frac{112.54\ kw}{3 * 153.57} = 244.27A.$$

The reactive power of DVR is QDVR = $3K_0V_{LP}$ IS $sin\delta$, $K_O = \frac{VLP}{VSsag} = \frac{220v}{153.57} = 1.43$ (3.37)

$$\delta = \sin^{-1}\frac{\text{QDVR}}{3\text{KOVLP Isag}} = \frac{65.85kvar}{3*1.43*220*244.27A} = \sin^{-1}0.285 = 16.55^0$$

The active power of DVR is:-

Pdvr = -3KoVsSagIssag (n_o – cosδ), $n_o = \frac{Vssag}{Vlp} = \frac{153.57v}{220v} = 0.7$, $\cos\delta = \cos(16.55^0) = 0.95$

Pdvr = -3*1.43*153.57*244.27(0.7-0.98) = 40.2322 kva.

The voltage rating of DVR is:-

$$V_{DVR} = V_{LP}\sqrt{1 + no^2 - 2no\ cos\delta} \quad (3.38)$$

$$V_{DVR} = 220\text{v}\sqrt{1 + 0.7^2 - 2 * 0.7\cos(16.55°)} = 88\text{v}.$$

The current rating of DVR is $I_{DVR} = I_S$ = 170.51A, since it connected in series with supply.

The KVA rating of DVR is $S_{DVR} = 3V_{DVR}I_{DVR}$ = 3*88v*170.51A = 45.01464 kva.

Voltage swell compensation

Afterward voltage swell, the source swell line voltage rises to: Vslswell = 380(1+0.1) = 418v and the supply swell phase voltage, $Vspswell = \frac{Vslswell}{\sqrt{3}} = 241.3v$.

The supply current during swell compensation is,

$$Isswell = \frac{Active\ power}{3Vspswell} = \frac{112.54kw}{3 * 241.3v} = 155.46A$$

The reactive power of DVR is,

$$QDVR = 3K_0V_{LP}\ IS\ sin\delta,\ K_0 = \frac{VLP}{VSswell} = \frac{220v}{241.3v} = 0.912 \quad (3.39)$$

$$\delta = \sin^{-1}\frac{QDVR}{3KoVLP\ Iswell} = \frac{65.85kvar}{3 * 0.912 * 220 * 155.46A} = \sin^{-1} 0.7 = 44.42°$$

The active power of DVR is:-

$$Pdvr = -3KoVsSwellIsswell\ (n_o - cos\delta\ ),\ n_o = \frac{Vsswell}{Vlp} = \frac{241.3v}{220v} = 1.11 \quad (3.40)$$

Pdvr = -3*0.912*241.3*155.46(1.11- cos(44.42)) = 40.6197kva.

The voltage rating of DVR is:-

$$V_{DVR} = V_{LP}\sqrt{1 + no^2 - 2no\ cos\delta} \quad (3.41)$$

$V_{DVR} = 220\sqrt{1 + 1.1^2 - 2 * 1.11\ \cos(44.42°)}$ = 176.85v.

The current rating of DVR is $I_{DVR} = I_S$ = 170.51A, since it connected in series with supply.

The KVA rating of DVR is $S_{DVR} = 3V_{DVR}I_{DVR}$ = 3*176.85v*170.51A = 90.4640 kva.

Hence, considering an overall rating (normal, voltage sags and swell), the rating of the compensators are:-

Max V_{DVR} = 176.85V, Max I_{DVR} = 244.27A

Therefore, the size or rating of the DVR will be:-

S=3 V_{DVR} I_{DVR} = 3*176.85V*244.27A = 129.59KVA, but EEU has not the rating of 129.59kva approximately 100kva would be the rating of DVR for compensation.

The turn ratio of the inject transformer for DVR is calculated as the following:-

$$\text{The DC bus voltage, } = \frac{2\sqrt{2}load\ voltage}{\sqrt{3}ma} \quad (3.42)$$

Where ma= modulation index = 1, $Vdc = \frac{2\sqrt{2}*380}{\sqrt{3}*1}$ = 620.54V ≈ 700V.

DVR needs only 176.85v per phase, Therefore the turn ratio of the inject transformer for DVR:-

$K_{DVR} = \frac{load\ voltage}{\sqrt{3}*Vdvr} = \frac{380v}{\sqrt{3}*176.85v} = 1.25 \approx 1$

The interface inductance of the DVR is, $L_{DVR} = \frac{\sqrt{3}}{2} \frac{maVdcKdvr}{6af\Delta Idvr}$ (3.43)

For 5% of the current ripple, $\Delta Idvr = Icr,pp = Idvr * 0.05 = 244.27A * 0.05 = 12.2135A$

$$L_{DVR} = \frac{\sqrt{3}}{2} \frac{700*1}{6*1.2*20000*12.2135} = 0.344mH.$$

Chapter Four

Result and Discussion

4.1 Introduction

To increase approximation coefficients and frequency resolution for details, decomposition is repeated up to several stages in MRA. By reconstructing the deconstructed signal using the up sampling process, DWT-MRA allows for the recovery of original time domain signals without sacrificing any information. An impulse-responsive half-band LP filter is applied to the sample waveform under study in MRA-based wave decomposition. The aim of decomposing and extracting of power quality problem is to convert the original error signals from its time domain to the energy form of the frequency domain. Each generated PQDs is divided into four levels in this investigation using the DWT filter (db4). Figure 4.1 are the findings for a subset of the PQDs.

4.2 Detection using WT Multi-Resolution Analysis (MRA)

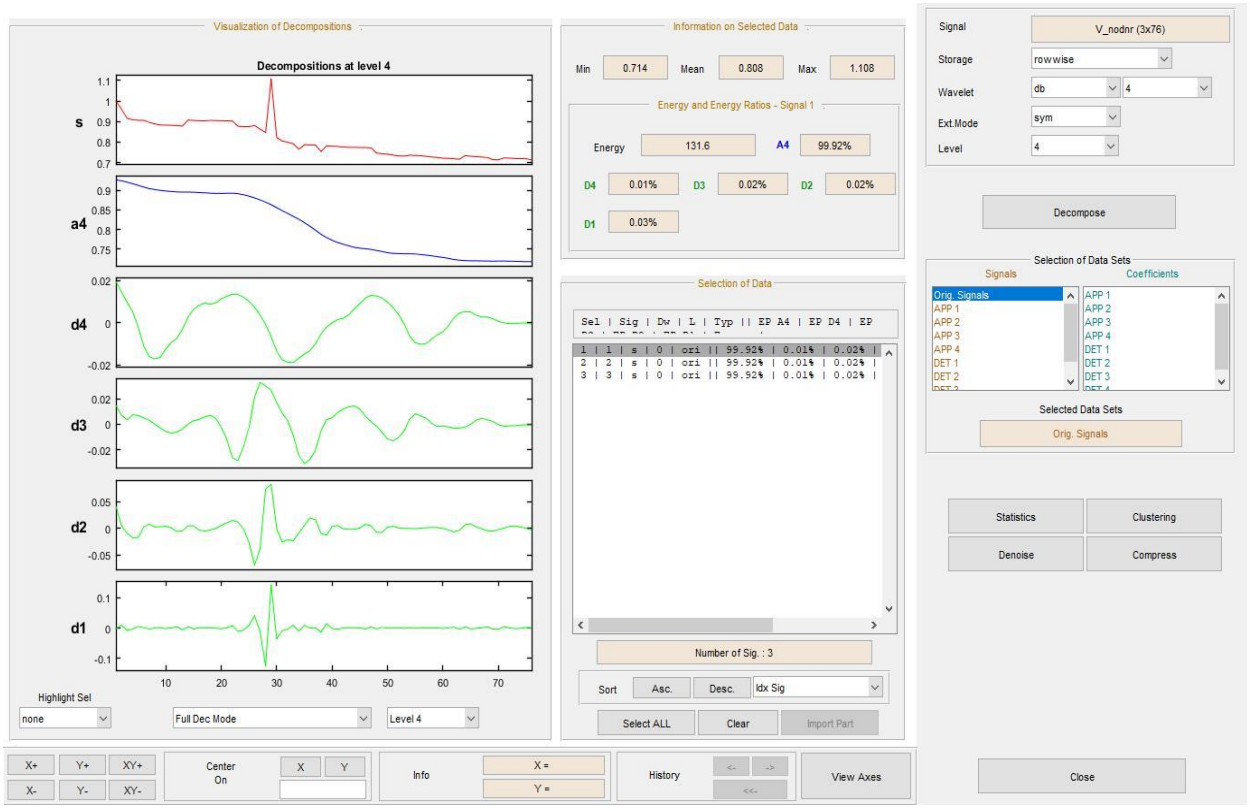

Figure 4. 1 Detection voltage sags and swells using WT (Multi-resolution Analysis)

As quantitatively mentioned, the output of five feature sets are showed for both the detailed coefficients (D) and the approximation coefficient (A), with an over-all of two feature set signals for each disturbance. Depending on how energetically they are structured, each higher frequency component is prioritized first, followed by lower frequency features. The feature sets selected for the classifier's training phase are the detailed feature sets. As a result, 5 × 2 (two distorted, or sag + swell) signals yield 10 characteristics. Each of the disturbances is depicted as having a random values at each generation based on its numerical features.

Table 4. 1 The eight classes of signals Extracted from Multi-resolution Analysis

Signal	Energy	A 4	D 4	D 3	D 2	D 1	Min	Mean	Max
Sag and Swell	131.5	99.92	0.01	0.02	0.02	0.03	0.714	0.809	1.108

4.3 Detection using S-Transform

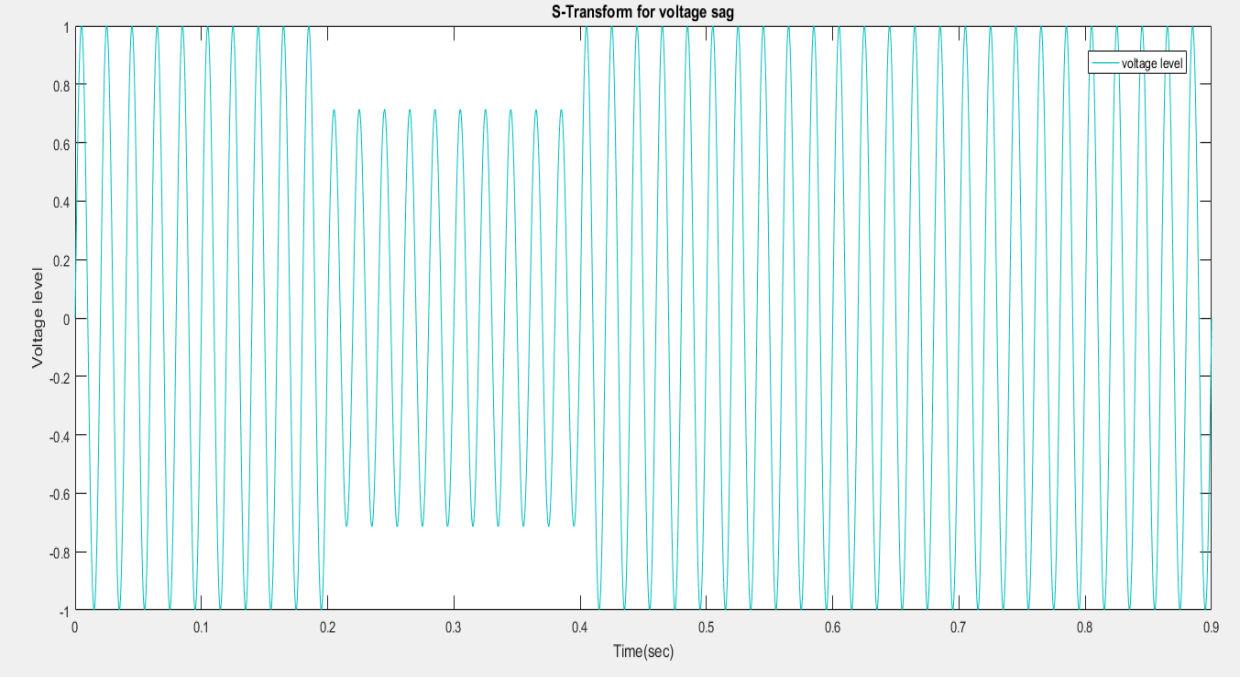

Figure 4. 2 Voltage Sag Detection Using S – Transform

In the figure 4.2, the S-transform is normalized to have values between 1 and -1. This normalization helps to standardize the results and make them more comparable across different signals. The range of 0.714 to -0.714 captures significant deviations from the nominal voltage level. Voltage sags, which are characterized by a sudden decrease in voltage, often fall within this range. This range provides a balance between sensitivity (detecting true voltage sags) and specificity (avoiding false positives). A wider range might capture more noise or other insignificant variations, while a narrower range could miss subtle voltage sags.

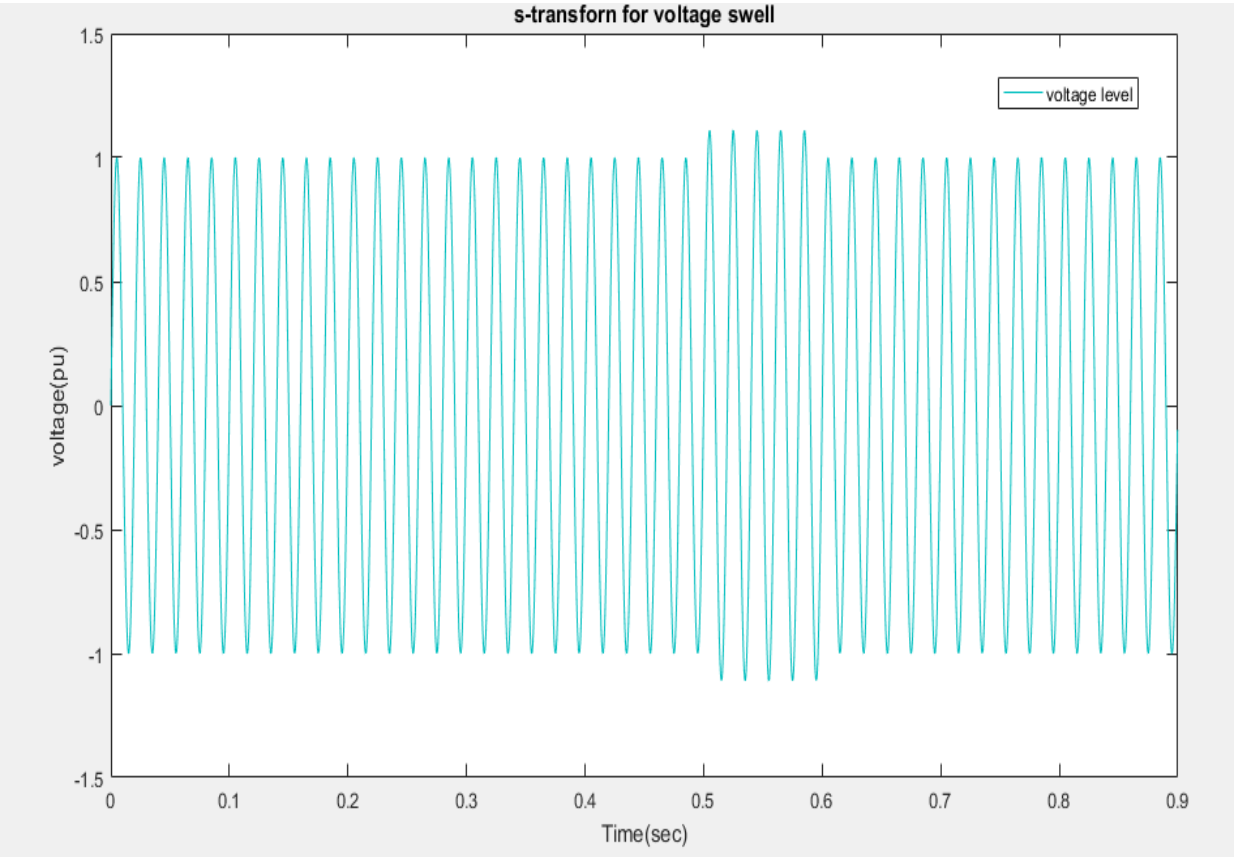

Figure 4. 3 Voltage Swell Detection Using S – Transform

In the figure 4.3, S-transform is a time-frequency analysis technique that can be effectively used for detecting voltage swells in power systems at a range of 1.11 to -1.11. Voltage swells are characterized by a sudden increase in voltage. By extending the range beyond the typical 1 to-1 normalization, the S-transform becomes more sensitive to these significant deviations from the nominal voltage level.

4.4 Comparison between WT and ST

Table 4. 2 Comparison between WT and ST

Feature	Wavelet Transform	S-Transform
Energy Distribution	Signals with energy content.	Signals without energy content.
Decomposition and Approximation	Decomposes the signal into a series of approximations and details coefficients at different scales.	Does not explicitly decompose the signal into approximations and details.
signals	Analyse signal multiples stage.	Less analyse signal.

4.5 Classification of Power Quality Disturbances Event using ANN

- Number of layers:- 3 (Input, hidden and output)
- Number of neurons in input layer:- 10
- Number of neurons in the output layer: -1
- Data division: random (dividerand)
- Activation function for output layer: LEARNGDM
- Training algorithm: Lavenberg-Marquardt(TRAINLM)
- Number of input variables: 1(76 bus voltage)
- Number of hidden neuron: this was adjusted until the optimum training performance was obtained. The designed ANN model is as shown in, as obtained from MATLAB at the time of the training/simulation

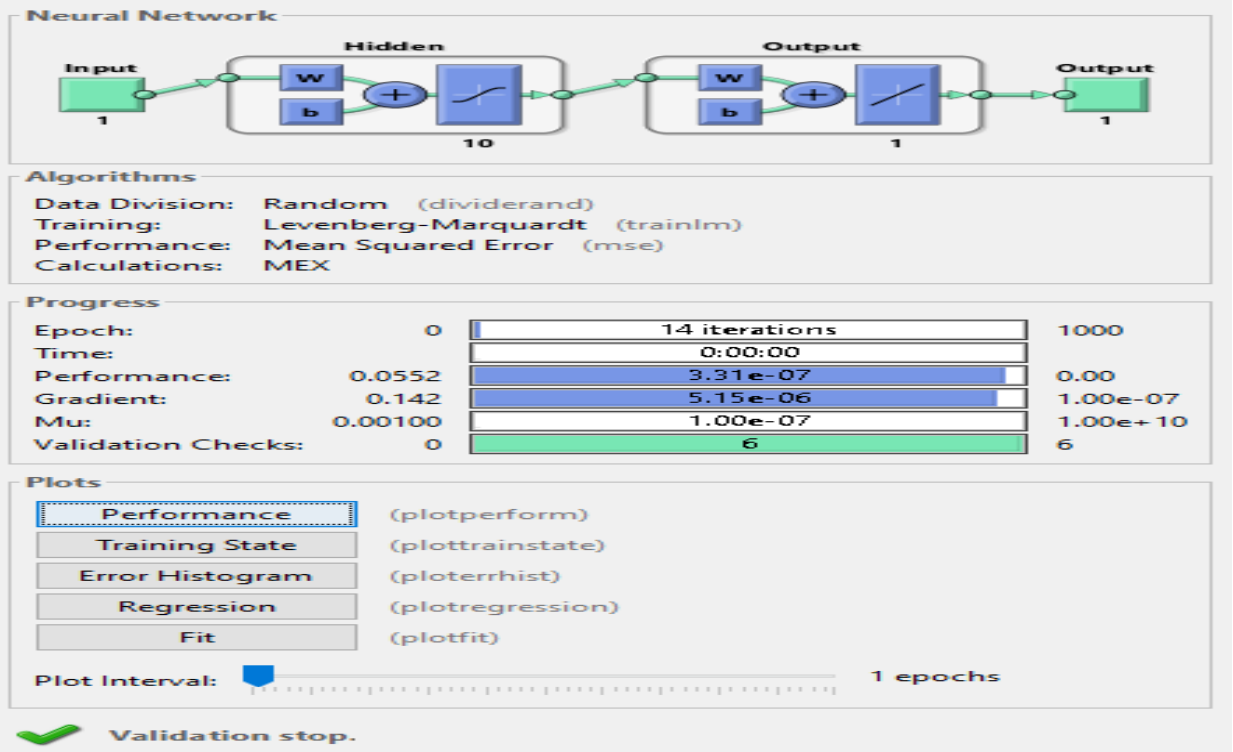

Figure 4. 4 Matlab Training tool interface and neural network architecture.

Table 4. 3 The ANN predicted features of two classes signal

Bus No.	v (pu)	Bus No.	v (pu)
1	1	39	0.782298112
2	0.960456759	40	0.780347754
3	0.916340407	41	0.779261301
4	0.908879679	42	0.775953178
5	0.906257503	43	0.774790691
6	0.906128914	44	0.774472989
7	0.896411242	45	0.773906882
8	0.888506126	46	0.773467767
9	0.883930065	47	0.773129478
10	0.882529604	48	0.747135434

11	0.882021214	49	0.744151329
12	0.88077918	50	0.740845182
13	0.878132563	51	0.736968926
14	0.907783733	52	0.733130831
15	0.90573535	53	0.731934434
16	0.904181765	54	0.736963288
17	0.903865838	55	0.734964846
18	0.905930425	56	0.734250411
19	0.905215699	57	0.730344477
20	0.904747161	58	0.72763514
21	0.903824965	59	0.725451589
22	0.903391404	60	0.721479582
23	0.877158235	61	0.720818459
24	0.87563244	62	0.719037308
25	0.875532077	63	0.716271248
26	0.881112663	64	0.734601008
27	0.863395476	65	0.731240219
28	1.099912222	66	0.729270978
29	0.835583379	67	0.727220677
30	0.822529997	68	0.725320105
31	0.805140364	69	0.715121738
32	0.800128625	70	0.714091864
33	0.791600591	71	0.723212748

34	0.765693157	72	0.721945953
35	0.786835756	73	0.720288127
36	0.786269691	74	0.719632482
37	0.785778615	75	0.719086443
38	0.754126654	76	0.714538471

The average performance accuracy of an LSTM is 100%. Its high accuracy leads us to conclude that the categorization performance is excellent. A database generates PQDEs, and an FFNN classifier is implemented using a random sample. Base case data from load flow analysis is inspected, evaluated, and trained to ascertain the correctness of each disturbance as well as the overall accuracy. The classifier's accuracy of over 99% demonstrates the effectiveness of DWT-ANNs for power quality problems.

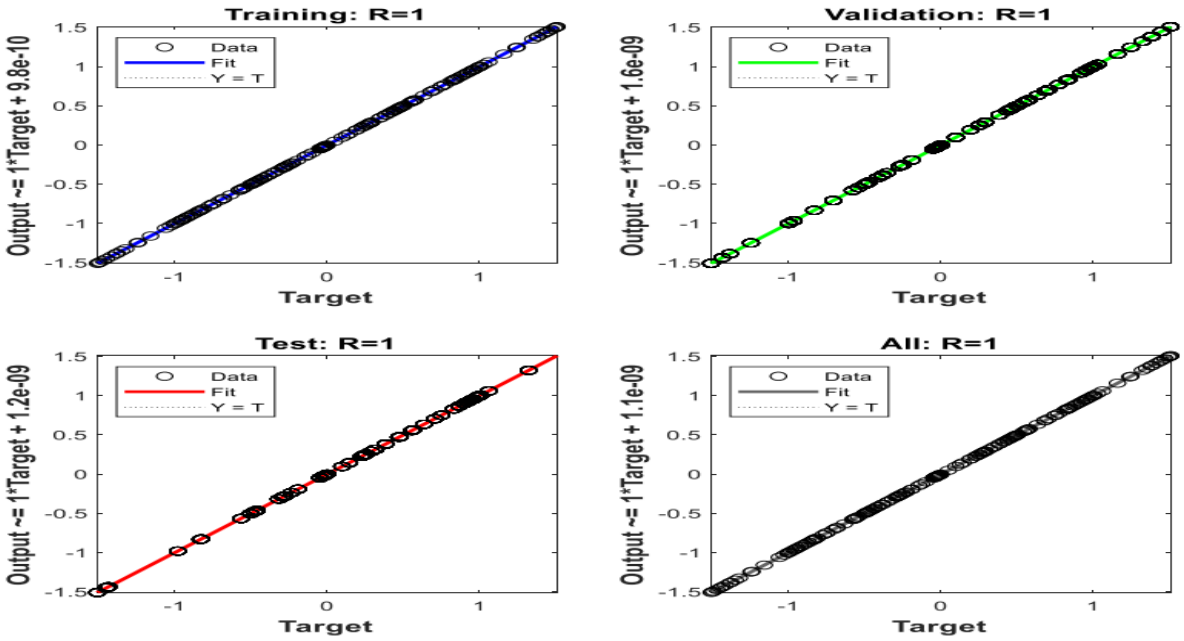

Figure 4. 5 The regression results of Training, Validation, and Test

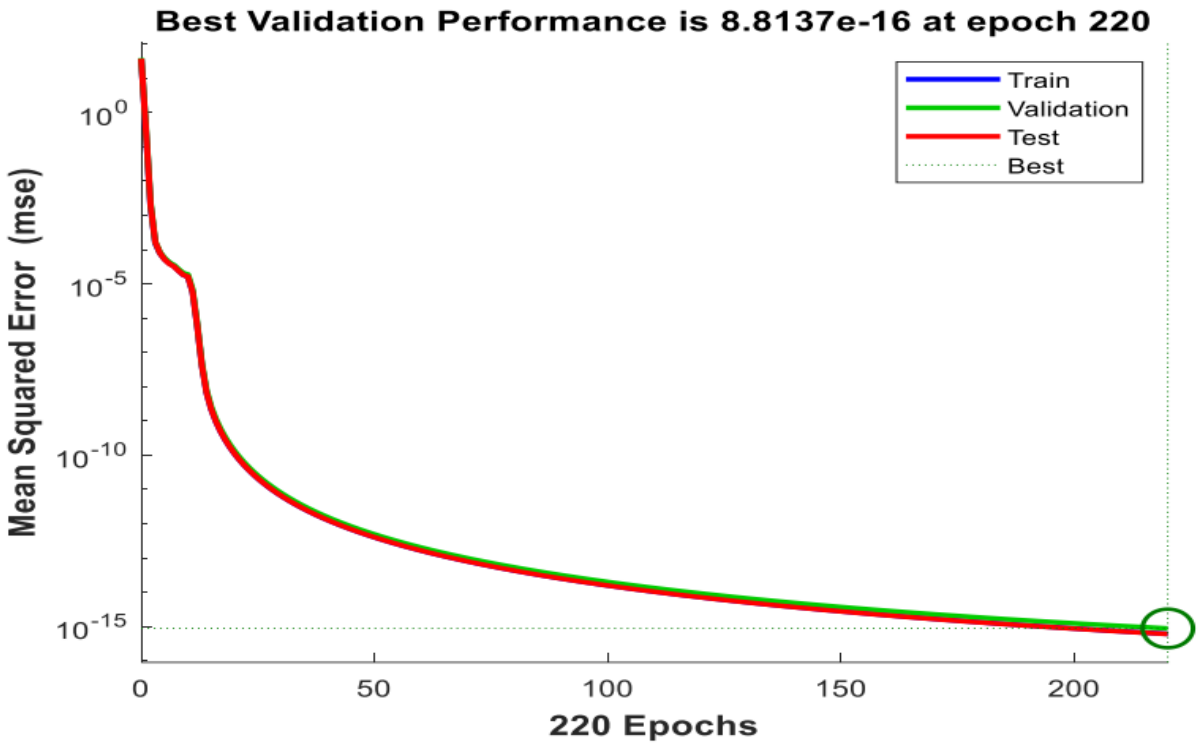

Figure 4. 6 Validation Performances of ANN

4.5 Classification performance in the Confusion Matrix

By using the graphic user interface (GUI) of confusion matrix to check how the certain classifier's executed in every class. The confusion matrix can be used to classify the areas in which the classifier has done well and poorly. The confusion matrix of three signals using the medium tree, boosted tree, and SVM classifiers is shown in the following. The anticipated class is shown in columns, whereas the true class is shown in rows. Where, the diagonal cells show that the true class and the anticipated class match. If these cells are green, the classifier has performed well and correctly classified observations of this true class. The default view shows the number of observations in each cell. To see the classifier's performance per class, select the True Positive Rates, False Negative Rates option under Plot. Each true class's summary is shown in the last two columns on the plot's right. To find areas where the classifier performed poorly, look at the red, high percentage-displaying diagonal cells. The greater proportion the brighter the color of the cell. In these red cells, the anticipated class and the true class are not the same. The data points have been misclassified.

4.5.1 Confusion Matrix of three classes by using boosted Tree.

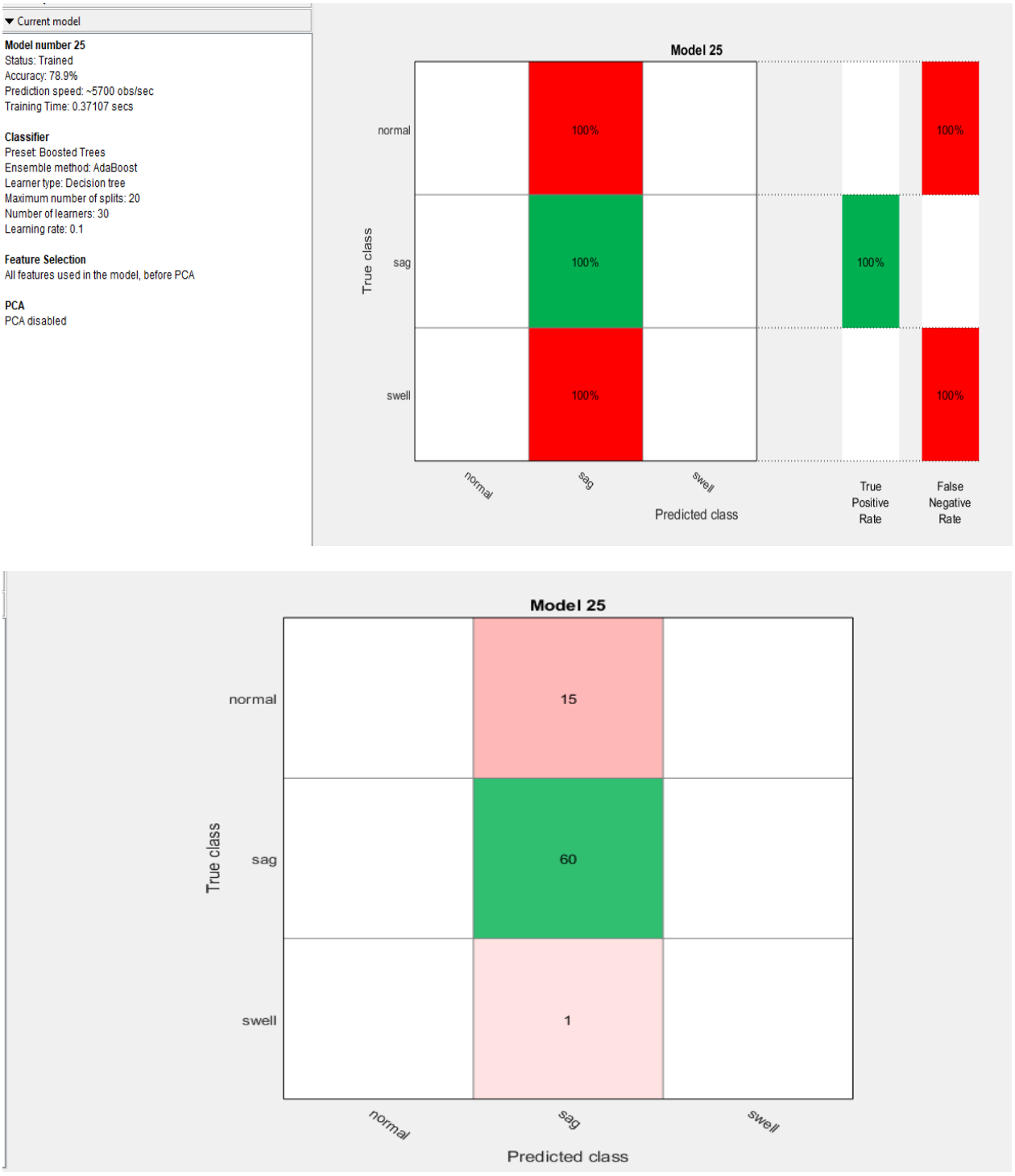

Figure 4. 7 Classification of three classes by using boosted Tree Classifier.

- In the figure 4.7 the accuracy of classifier is 78.9%.

4.5.2 Confusion Matrix of three classes by using Medium tree.

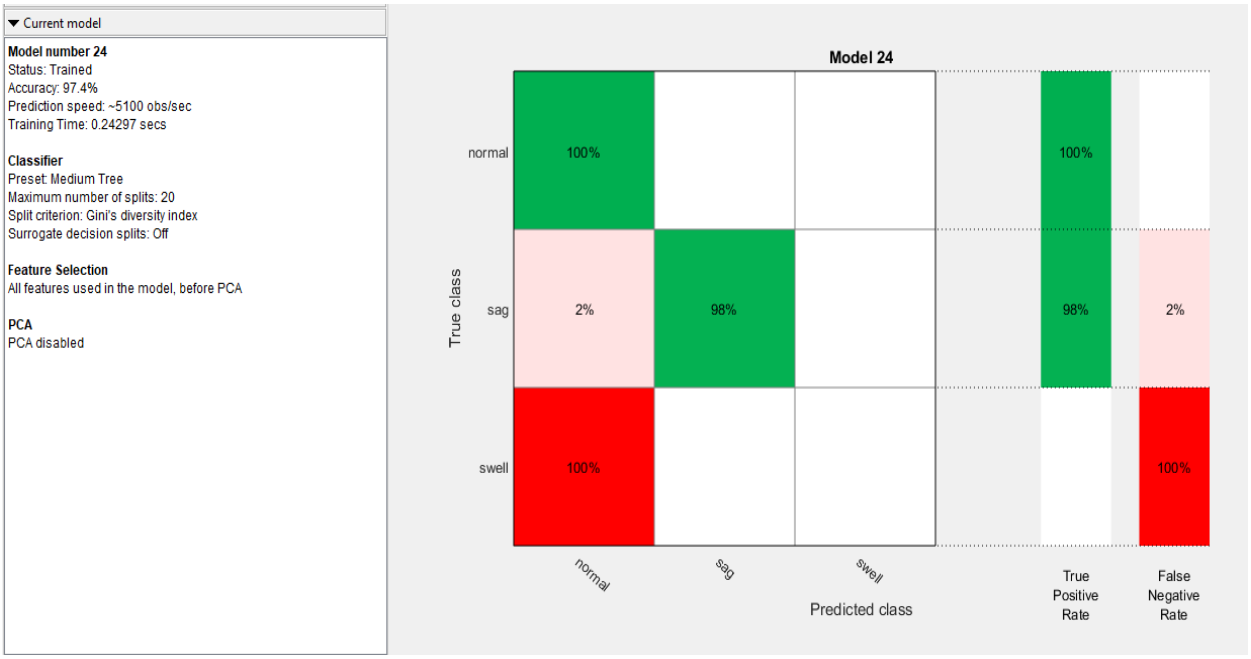

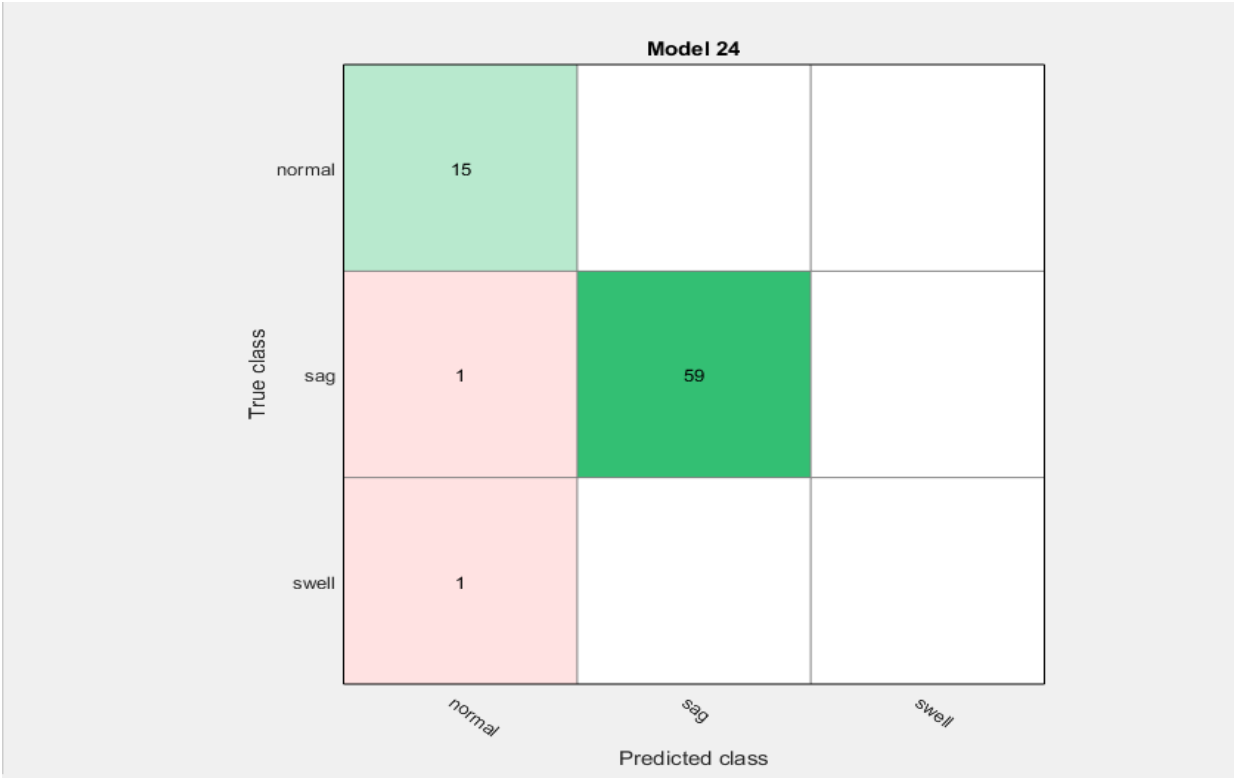

Figure 4. 8 Classification of three classes by using medium Tree Classifier

- In the figure 4.8 the accuracy of classifier is 97.4%.

4.5.3 Confusion Matrix of three classes by using SVM (Support Vector Machine).

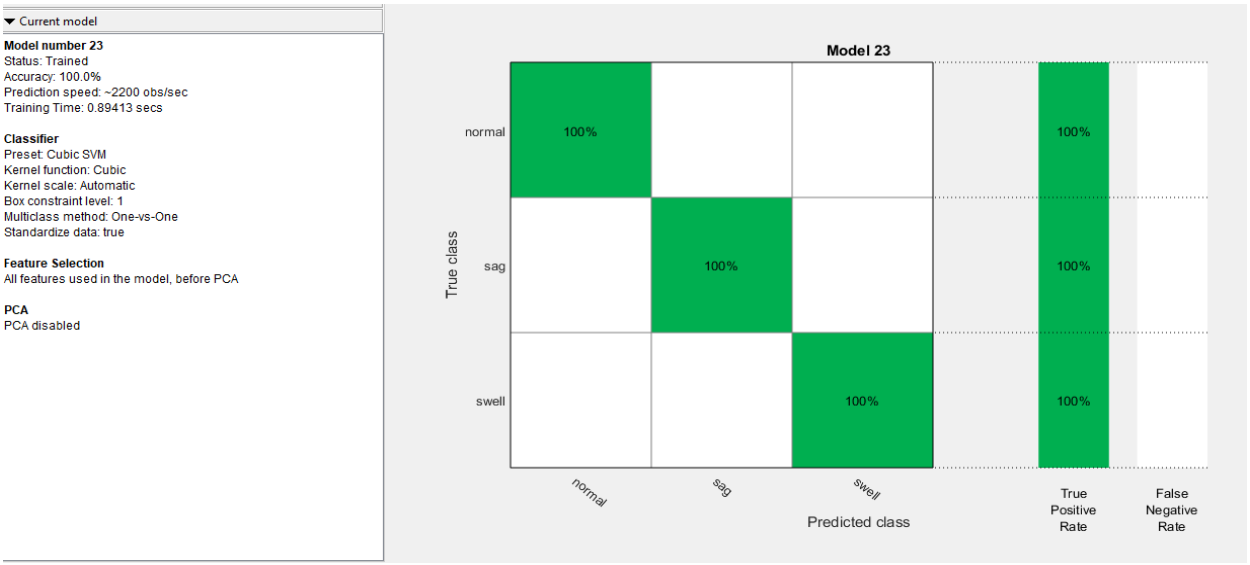

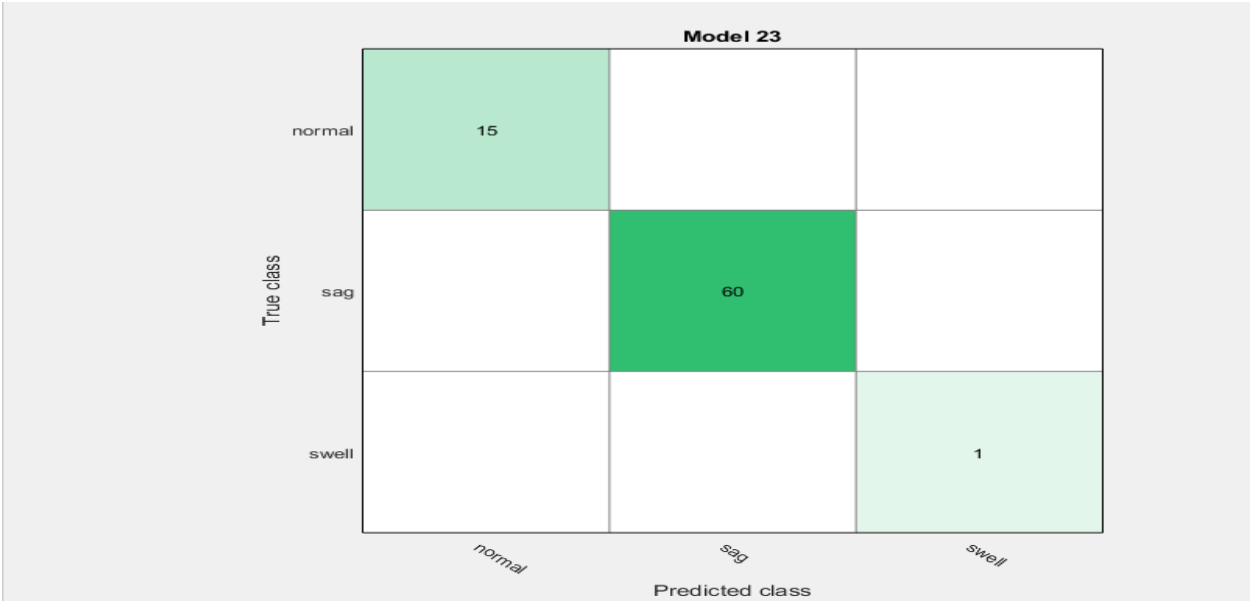

Figure 4. 9 Classification of three classes by using SVM Classifier.

- ✓ In the Figure 4.9 the accuracy of classifier is 100%.

The entire green rectangle (cells) in the true positive rate columns of each model indicates the true positive rate, which is represented by the percentages for successfully categorized points in this class. Of the PQDEs in the class, 78.9% (boosted), 97.4% (medium tree), and 100% (SVM) are correctly classified in the top row. The false negative rate for incorrectly categorized points in this class is represented by the percentages in the red cell of the False Negative Rate column.

Choose the number of observations under Plot if we would prefer to view PQDEs (numbers of observations) rather than percentages.

4.6 The ROC Curve (Receiver Operating Characteristic Curve)

Once a model has been trained, choose the ROC Curve from the Classification Learner tab's Plots section. Examine the receiver operating characteristic (ROC) curve to see the true and false positive rates. The ROC curve shows the true positive rate versus the false positive rate for the learned classifier that is currently chosen. We can map a lot of classes. The performance of the currently chosen classifier is shown by the plot's marker. The marker shows the currently selected classifier's true positive rate (TPR) and false positive rate (FPR) values.

The area under the curve number is a measure of the classifier's overall quality. Greater area under curve values indicates better classifier performance.

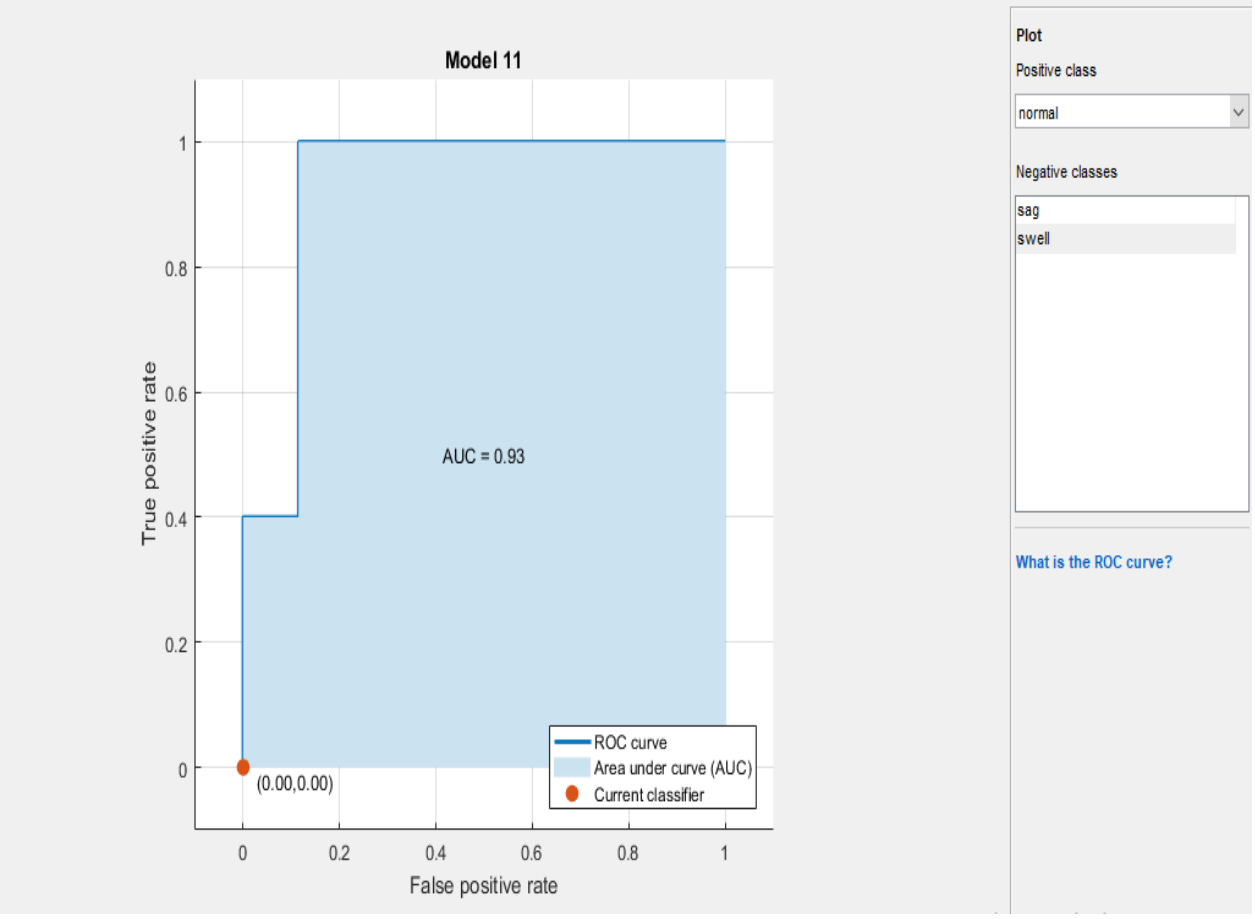

Figure 4. 10 Receiver Operating Characteristic (ROC) using Boosted Tree Mode

As an illustration, Area under Curve (AUC) of 0.93 in Figure 4.10 shows that 93% of the classifier performance present.

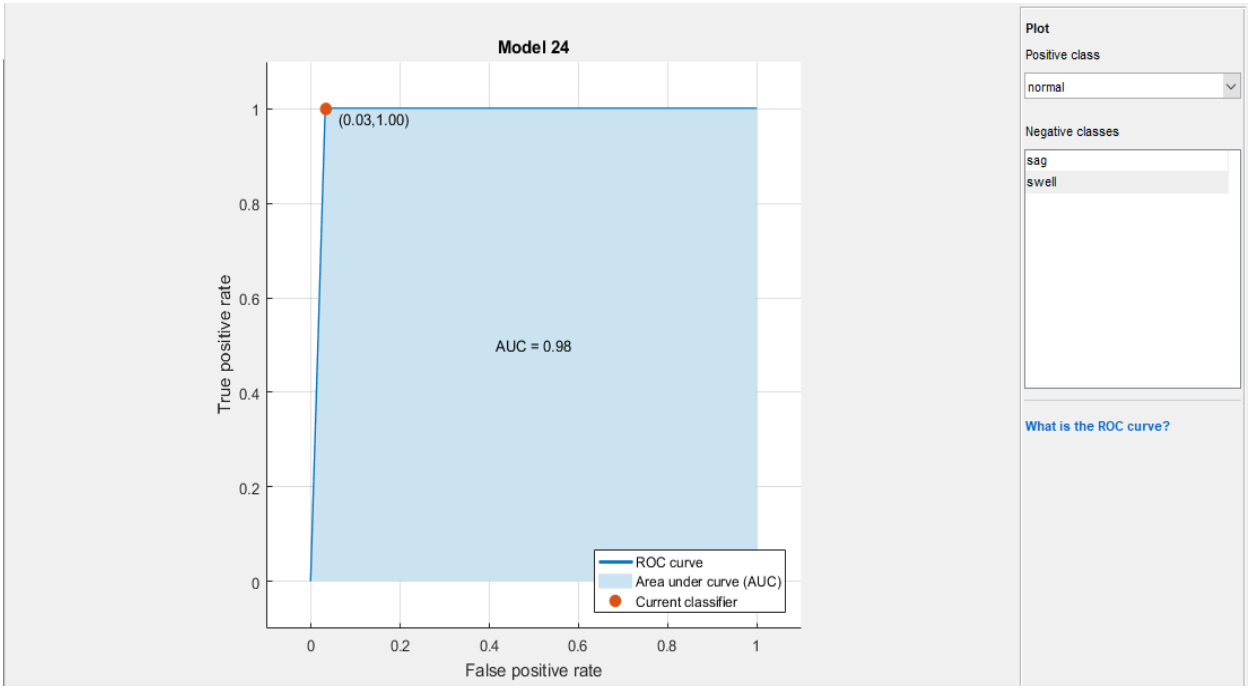

Figure 4. 11 Receiver Operating Characteristic (ROC) using Medium Tree Mode

In Figure 4.11 shows that Area under Curve (AUC) of 0.98 OR 98% of the classifier performance present.

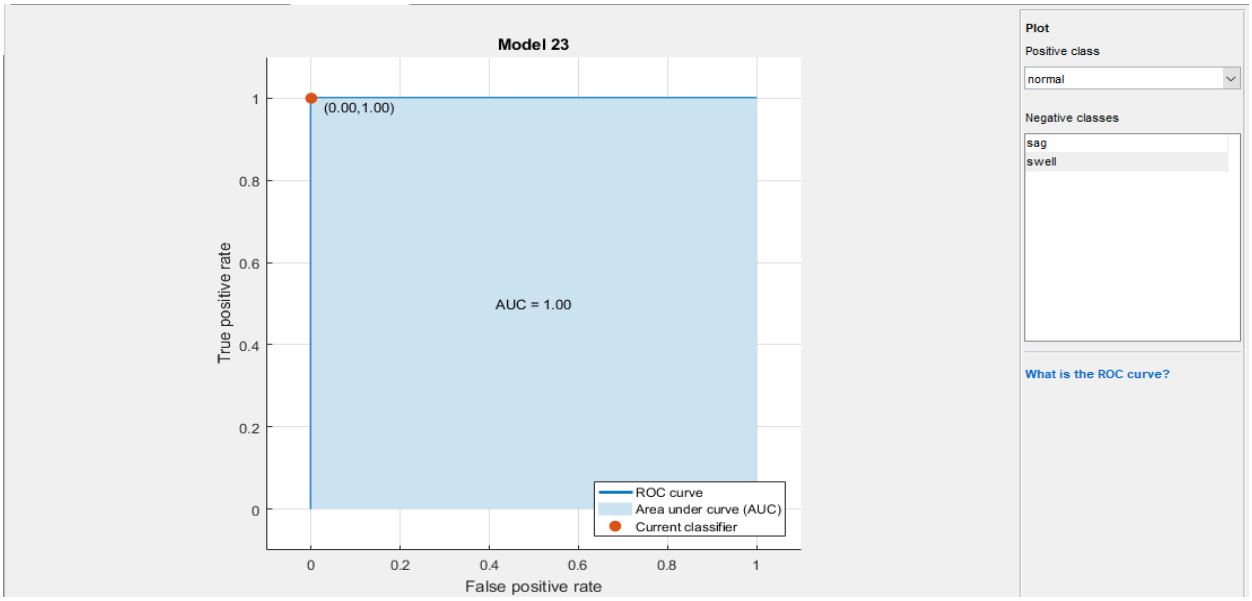

Figure 4. 12 Receiver Operating Characteristic (ROC) using SVM Mode

A straight angle to the upper left of the figure, as shown in Figure 4.12, indicates a perfect outcome with no misclassified dots. In table 4.4 ANN and SVM classify voltage sag, voltage swell and normal voltage profile of 76 bus to bus voltage profiles correctly and medium tree and boosted tree from the 76 bus classify the disturbance 97.4% and 78.39% respectively.

Table 4. 4 Comparison between classifiers

Classifier	accuracy	Rank
ANN	100%	1
Boosted Tree	78.9%	3
Medium Tree	97.4%	2
Support vector machine	100%	1

4.7 Mitigation Simulation Results and Discussion

Three scenarios were examined to determine the highest decrease in overall power losses, voltage profile improvement and cost in hawassa Distribution Feeder 6(R4-G5).

Scenarios I: Results for base case

Scenarios II: Voltage profile improvement using DVR+GOA

Scenarios III: Voltage profile improvement using DVR+PSO

4.7.1 Scenario I: Results for base case

4.7.1.1 Bus voltage

Before DVR, the load flow analysis based on backward/forward sweep (BFS) was carried out, and the bus voltage magnitudes are reported. Considered base voltage power values are 15 kV. Table 4.5 displays the bus voltage profile of the existing system.

Table 4. 5 Base case Profile of Voltage for The Feeder 6(R4-G5) Network

Bus No.	Base case v (pu)	Bus No.	Base case v (pu)
1	1	39	0.782298112
2	0.960456759	40	0.780347754
3	0.916340407	41	0.779261301
4	0.908879679	42	0.775953178
5	0.906257503	43	0.774790691
6	0.906128914	44	0.774472989
7	0.896411242	45	0.773906882
8	0.888506126	46	0.773467767
9	0.883930065	47	0.773129478
10	0.882529604	48	0.747135434
11	0.882021214	49	0.744151329
12	0.88077918	50	0.740845182
13	0.878132563	51	0.736968926
14	0.907783733	52	0.733130831
15	0.90573535	53	0.731934434
16	0.904181765	54	0.736963288
17	0.903865838	55	0.734964846
18	0.905930425	56	0.734250411
19	0.905215699	57	0.730344477
20	0.904747161	58	0.72763514
21	0.903824965	59	0.725451589
22	0.903391404	60	0.721479582

23	0.877158235	61	0.720818459
24	0.87563244	62	0.719037308
25	0.875532077	63	0.716271248
26	0.881112663	64	0.734601008
27	0.863395476	65	0.731240219
28	1.1099912222	66	0.729270978
29	0.835583379	67	0.727220677
30	0.822529997	68	0.725320105
31	0.805140364	69	0.715121738
32	0.800128625	70	0.714091864
33	0.791600591	71	0.723212748
34	0.765693157	72	0.721945953
35	0.786835756	73	0.720288127
36	0.786269691	74	0.719632482
37	0.785778615	75	0.719086443
38	0.754126654	76	0.714538471

At bus 76, it is found that 0.714 pu is the minimum bus voltage value. The bus voltage profile regarding the base case scenario load flow analysis is displayed in Table 4.5. It can be seen, the bus voltage magnitudes decrease as a result of non-linear loads.

4.7.2 Scenarios II: Voltage profile improvement using DVR+GOA

The network is optimized based on the initial loops of the proposed system using the GOA approach and the control parameters for the best DVR (dynamic voltage restorer) placement and sizing. The best location (position) for the DVR is at bus 29,35,40,53 and 66, which has a size of 100 kVA, as determined by repeatedly running the GOA algorithm in Matlab.

Table 4. 6 Initial Loops

Loop 1: - 5, 6, 7, 8, 11, 12, 22, 23, 24.
Loop 2:- 31, 32, 34, 35, 36, 38, 39, 40, 41, 42, 43, 44, 45, 46.
Loop 3:- 47, 48, 53, 54, 56, 57, 58, 59, 60, 61, 62, 68, 69, 75.
Loop 4:- 49, 50, 51, 52, 53, 63, 64, 65, 66, 67, 70, 71, 72, 73, 74,76.

Table 4. 7 GOA Parameters Used for DVR

Quantities of Swarm	20
The size of search space	4
W_{min} and W_{max}	[0.4, 0.9]
Maximum repetition	50
C_1 and C_2	[0.04, 1]

4.7.2.1 Bus voltages for GOA-based DVR

The widely recognized GOA control parameter selection determines which of these dimensions may produce the greatest outcomes, as indicated in Table 4.5. The GOA algorithm is repeatedly run in MATLAB with the aforementioned control settings in order to determine the ideal DVR placement and size. The findings are displayed for the feeder's bus voltage profile under DVR after the load flow is executed based on the dynamic voltage restorer. The bus voltage profile after DVR employing GOA case load flow analysis is shown in Figure 4.13.

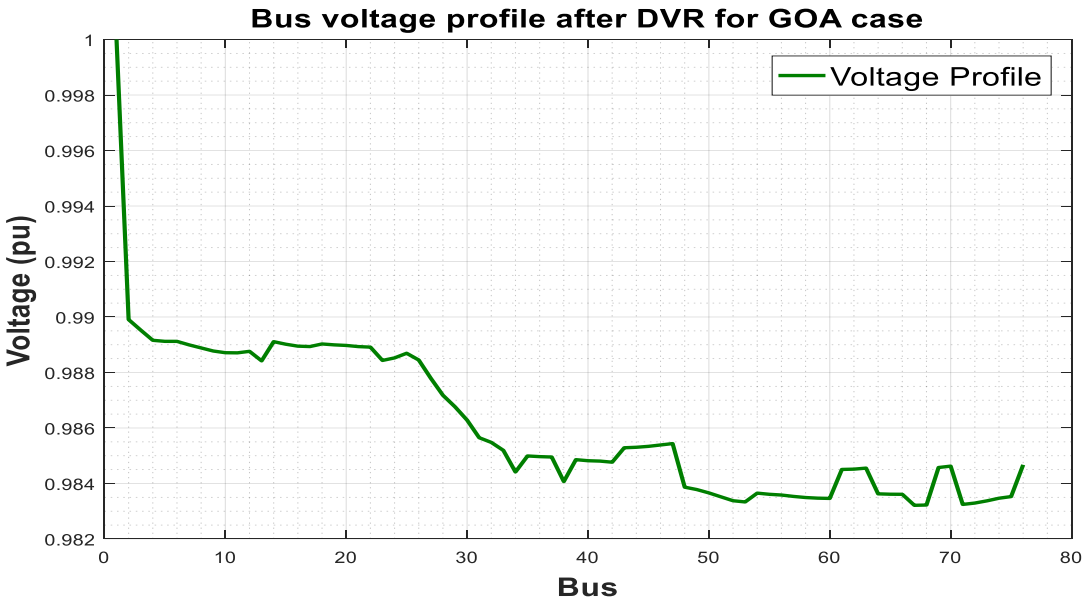

Figure 4. 13 bus voltage profile after DVR with GOA case

In the figure 4.13 displays the bus voltage profile following dynamic voltage restorer using GOA case with the minimum voltage of 0.98331(pu) recorded on bus 53. Figure 4.14 compares the bus voltage magnitude before and after DVR with GOA.

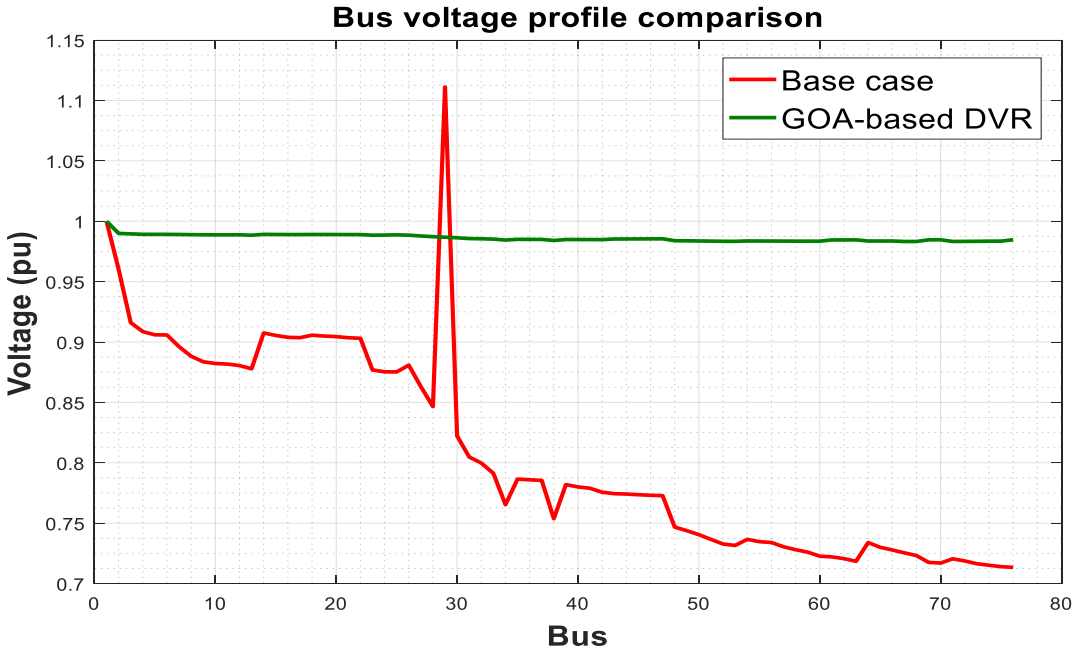

Figure 4. 14 bus voltage profile comparison for GOA case

As can be seen, in the GOA-based Dynamic Voltage Restorer scenario, the voltage magnitude of each bus has improved remarkably.

4.7.3 Scenarios III: Voltage profile improvement using DVR+PSO

Using the PSO method and the control parameters listed in table for optimal sizing and placement of DVR (dynamic voltage restorer), the network is optimized according to the suggested system's initial loops.

Table 4. 8 PSO Parameters Used for DVR

Quantities of Swarm	20
The size of search space	4
W_{min} and W_{max}	[0.4, 0.9]
Maximum Repetition	50
C_1 and C_2	Rad [0, 1]

4.7.3.1 Bus voltage for PSO-based DVR

Figure 4.15 displays the bus voltage profile following DVR using PSO case load flow analysis.

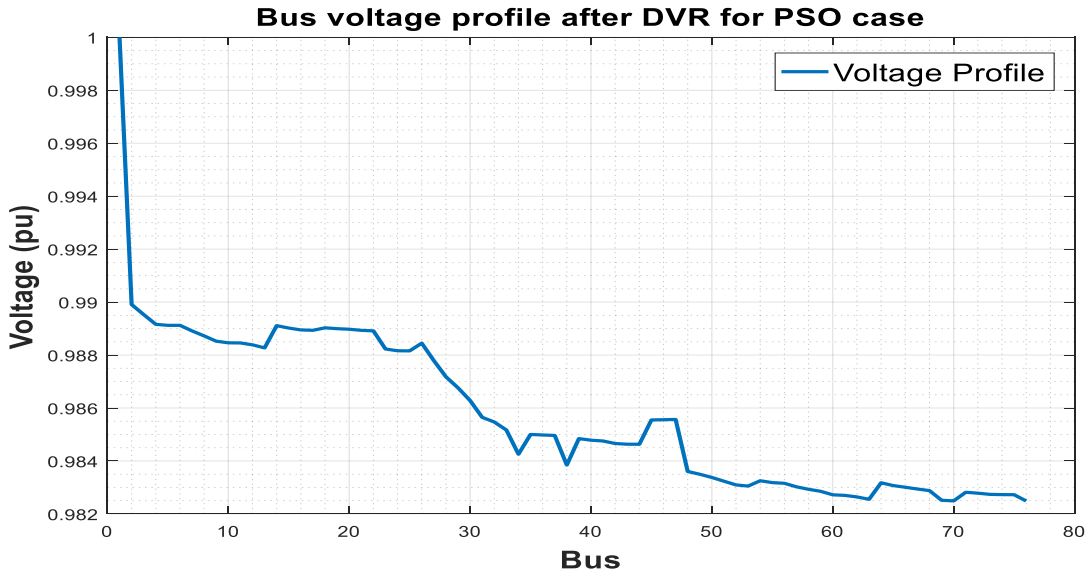

Figure 4. 15 bus voltage profile after DVR with PSO case

In the figure 4.15 displays the bus voltage profile following dynamic voltage restorer using PSO case with the minimum voltage of 0.9824 (Pu) recorded on bus 76.

Figure 4.16 compares the bus voltage magnitude before and after Dynamic voltage restorer. As Demonstrated, in the PSO-based DVR scenario, the voltage magnitude of each bus is much enhanced.

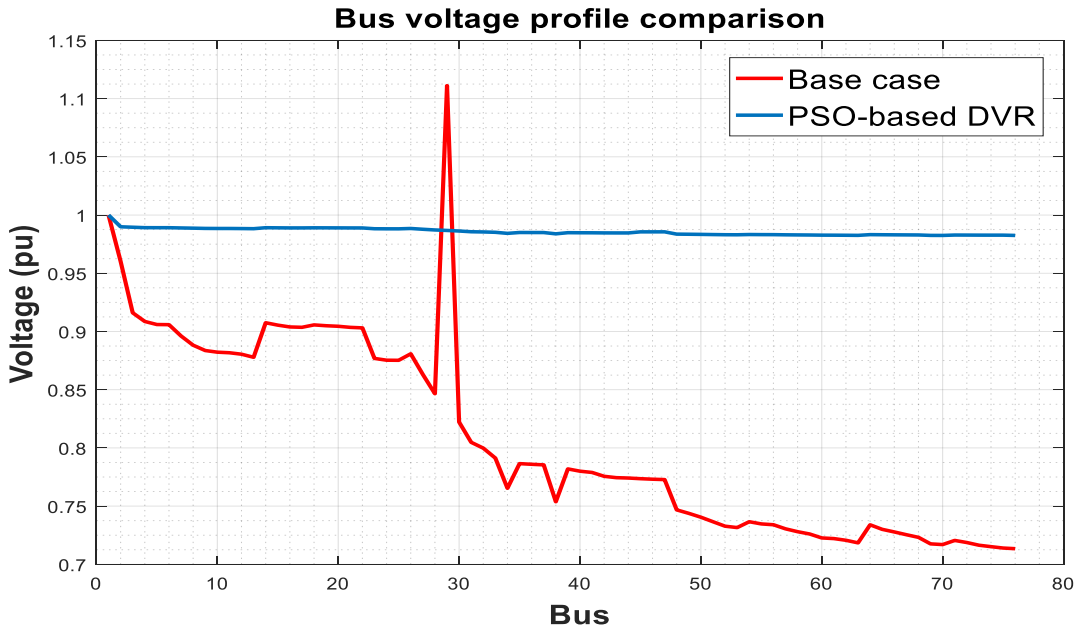

Figure 4. 16 bus voltage profile comparison for PSO case

4.8 GOA VS PSO Comparison

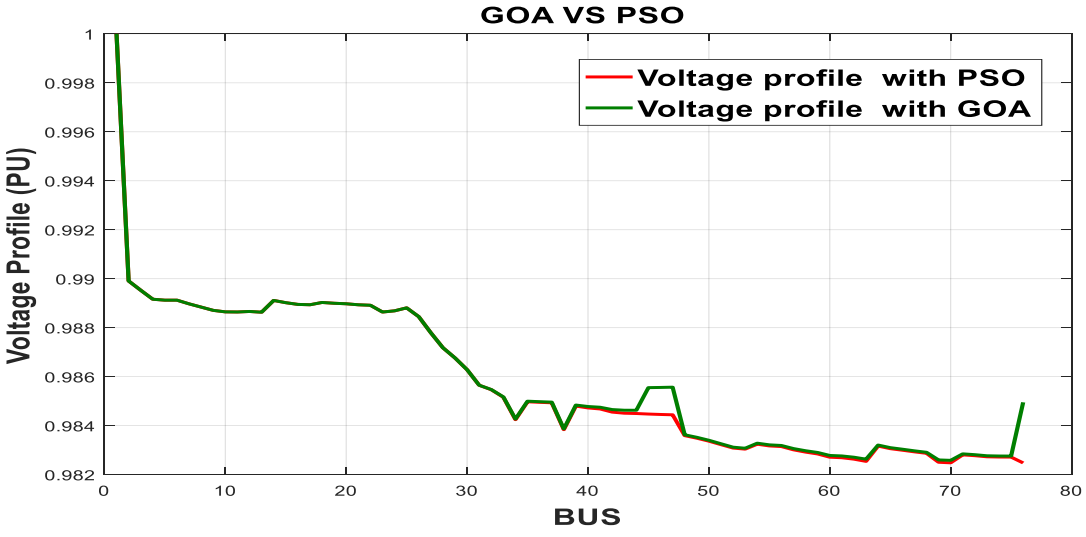

Figure 4. 17 comparison between GOA and PSO

Table 4. 9 Comparison of GOA and PSO with benchmark

Method	Min bus voltage(pu)	PT_{loss}(kw)	Elapsed time(sec)
Base case	0.714538471	1913.3	
GOA	0.983312544	286.817	2.020039
PSO	0.982442511	304.966	6.923559

4.9 Mitigation Results of Power Quality Disturbances Using Simulink DVR

The average resistance and reactance values are taken in a five-bus for each bus of power system model implemented in Simulink. Through simulations and analysis, the average resistance and reactance for specific bus within the system have been determined as follows: - bus 29 (0.852 + j0.159 per unit), bus 35 (0.492 + j0.295 per unit), bus 40 (0.550 + j0.331 per unit), bus 53 (0.463 + j0.278 per unit), and bus 66 (0.568 + j0.349). These average resistance and reactance values provide crucial insights into the characteristics of the power system network. The resistive components (0.852, 0.492, 0.550, 0.463 and 0.568 per unit) represent the energy losses within these elements due to the flow of real power. The reactive components (0.159, 0.295, 0.331, 0.278 and 0.349 per unit) indicate the opposition to changes in current and voltage, influencing the reactive power flow and voltage stability of the system.

The loads incorporated within a five-bus power system model developed in Simulink. Specifically, the model includes five distinct loads connected to different buses, with their active power (P) demands defined as follows: load 1 (at Bus 29): 931.3 kW, load 2 (at Bus 35) 311.87 kW, load 3 (at Bus 40) 686.4 kW, load 4 (at Bus 53) 630.5 kW and load 5 (at Bus 66) 324.46 kW To confirm DVR's functionality under sag and swell circumstances during faults, a thorough simulation was conducted using Simulink. Reduction of voltage sag during short circuit faults: Dynamic Voltage Restoration (DVR) systems can reduce voltage sags in the case of a short circuit fault. In order to keep voltage levels within reasonable bounds, these technologies reintroduce voltage into the grid. Reduction of voltage surge during line failures: line faults, such as lightning strikes or tree branches colliding with electrical wires, can result in voltage swells.

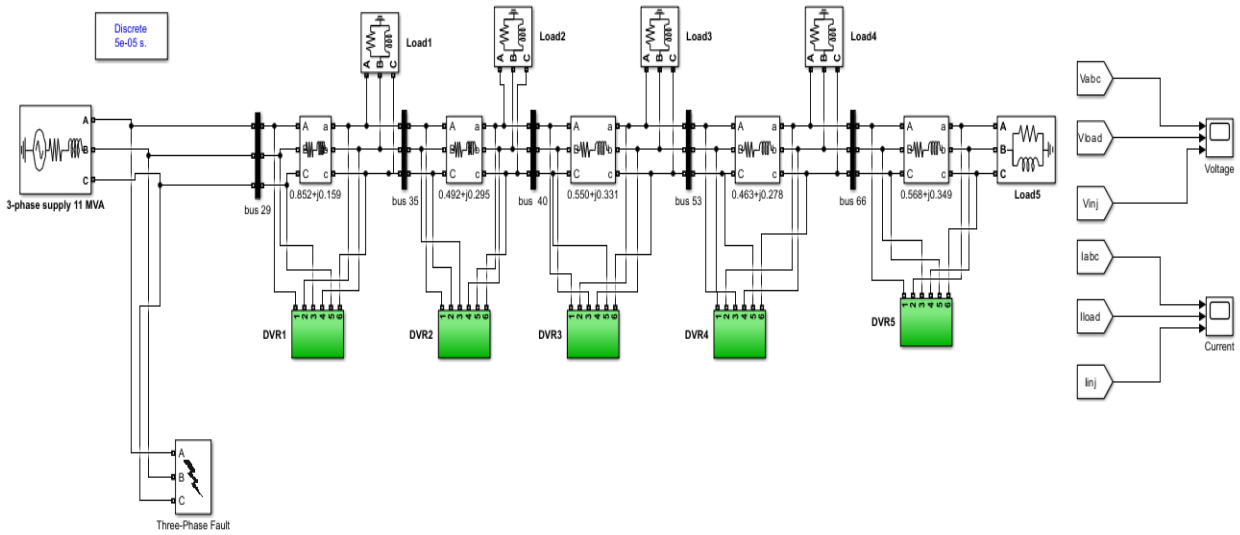

Figure 4. 18 Power quality disturbance mitigation

Before installing a DVR (Dynamic Voltage Restorer) on a distribution feeder 6, as clearly shown in the figure 4.19, a swell disturbance happens during faults. The feeder voltage was increased to 1.1 (pu) of its RMS value throughout the experiment, and this swell condition was meant to be used from 0.1 to 0.2 s. This swell case must be detected by the DVR to supply the necessary output voltage magnitude to maintain a stable and sinusoidal output. Between 0.3 and 0.4 seconds, there is a voltage drop and it dramatically drops to 0.3 (pu) of its initial value. Therefore the distorted waveforms observed without DVRs in Figure 4.19 results indicate the importance of implementing DVRs to regulate voltage levels and improve overall system stability.

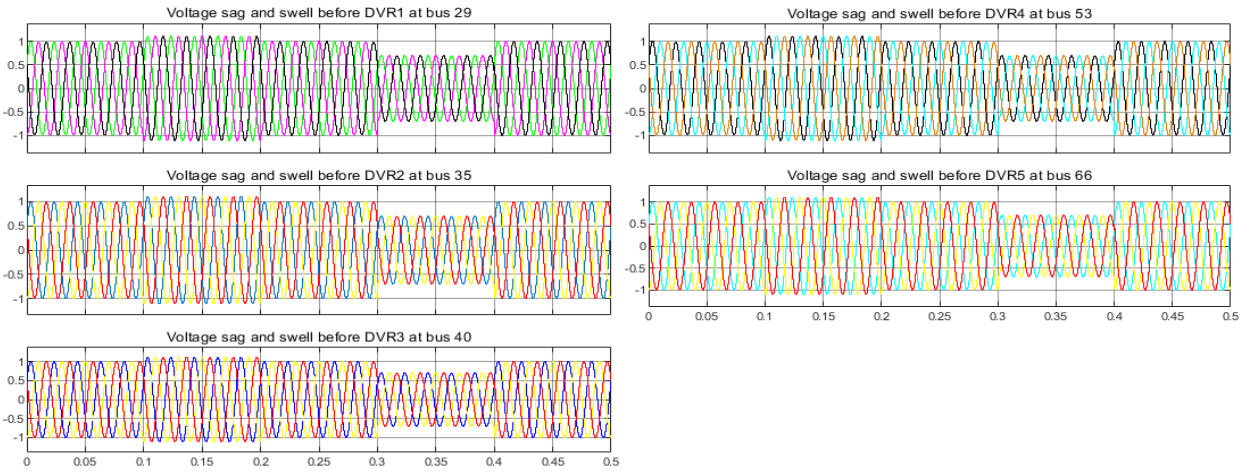

Figure 4. 19 Before DVR voltage sag and swell in distribution system

The Figure 4.20 shows waveform after mitigation by DVR at Vload showing the effect of a Dynamic Voltage Restorer (DVR) on voltage waveforms at different bus in the specific feeder six., these plots display smooth, balanced, and sinusoidal three-phase voltages, indicating that the five DVRs effectively compensate for voltage disturbances. To ensure the DVRs operate at their maximum potential, they were placed at their optimum locations (29, 35, 40, 53 and 66) within the system, as determined through thorough analysis. The consistency of the waveforms across all subplots indicates that the DVRs successfully restore voltage stability by mitigating sags and swell, during different fault conditions.

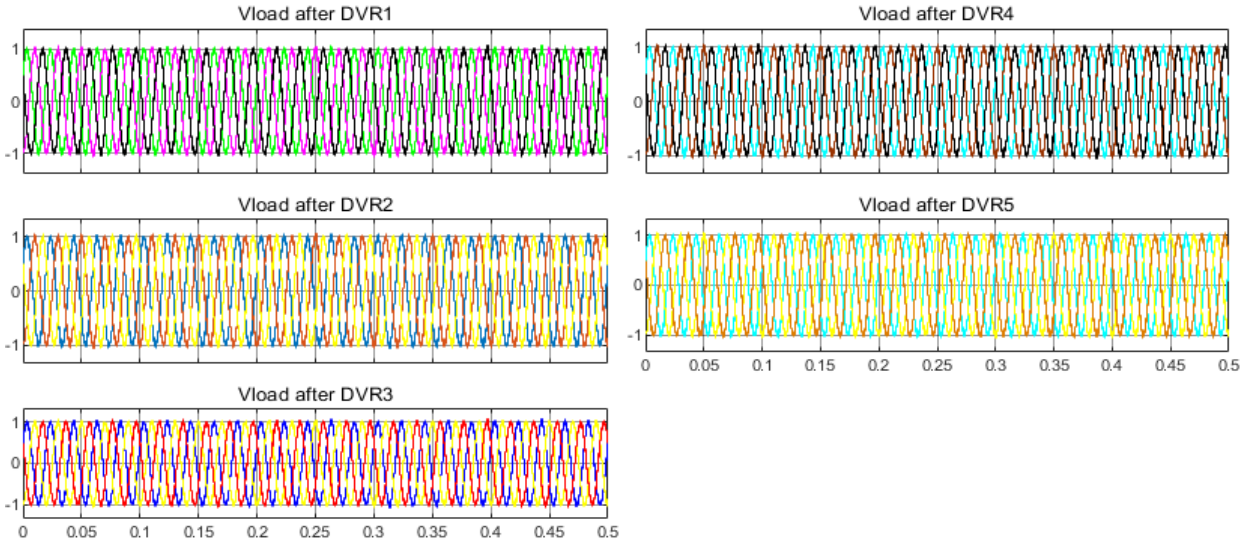

Figure 4. 20 mitigated Voltage sag and swell after installing DVR

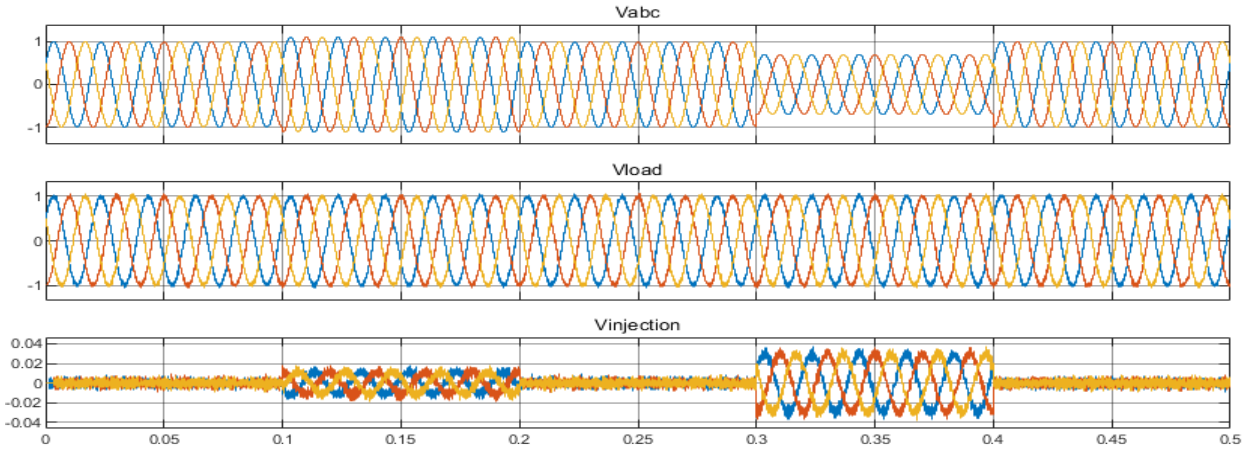

Figure 4. 21 over all the disturbed voltage, mitigated voltage, and injected voltage of Feeder 6(R4-G5).

In figure 4.21 as shown the voltage sag and swells are instantly detected by the DVR, which then supply the necessary output voltage magnitude for over all feeder six buses(76 bus) to maintain a stable and sinusoidal output. Table 4.10 shows why DVR is selected in this thesis rather than D-statcom.

Table 4. 10 DVR comparison with D-statcom

Parameters	**DVR**		**D-statcom (https://www.researchgate.net/publication/283350844)**	
Voltage improvement (PU)	Sag(Pu)	Swell(pu)	sag	swell
	0.714 to 1	1.11 to 1	0.793 to 0.95	1.146 to 1.02
Simulation time	0.1≤ts≤0.2	0.3≤ts≤0.4	0.25≤ts≤0.5	0.75≤ts≤1
Behaviour	Dynamic		Sluggish	

4.10 Cost analysis

Expenses for restarting operations and fixing any damaged equipment are included in the economic impact of power outages for small industrial clients, in addition to the cost of missed production. Commercial clients deal with comparable difficulties, including possible property damage and revenue losses from halted business activities. Financial hardships for residential customers also include ruined food and the requirement to use alternate energy sources during blackouts.

The costs of power outages for utilities like Hawassa Utility include labor, equipment, and replacement parts, among other expenditures involved with electricity restoration. In addition, utilities risk fines if they don't meet regulators' requirements for service reliability. Hawassa Utility may make more informed decisions on infrastructure maintenance and investment by employing the Expected Energy Not Supplied (EENS) metric to more accurately forecast the expenses related to power outages. Before DVR, the Hawassa distribution system experienced a power loss of 1913.3 KW; with the GOA optimization approach, this power loss is decreased to 295.534 KW.

Before DVR

Ploss=1913.3KW and Qloss=1202.4Kvar from load flow analysis.

Per year Kwh Loss:-

1913.3kw*8760h= 16,760,508 kwh.

Utility price is 3.35 birr /kwh So, 16,760,508 kwh*3.35 birr/kwh=56,147,701.8 birr or 452,329.83 $ annual loss.

After DVR

Ploss=295.534 kw and Qloss=261.803kvar.

Per year Kwh Loss:-

295.534kw*8760h=2,588,842.8kwh

2588842.8kwh *3.35 birr/kwh =8,672,623.38 birr or 69,867.26$ annual loss.

The Hawassa distribution system collected data on fault and load during disruptions to determine the necessary rating for the dynamic voltage restorer. Currently, the cost of a DVR is around $300 per kVA on average, which should be higher or equal to the gathered scores for fault and load.

The DVR expense for 100kva =100*300$= 30,000$

Installation cost 10% of 30,000 $ = 3000$

Maintenance cost 2% 0f 30,000$= 600$

Total investment cost = Cost of dvr + Installation Cost + Maintenance Cost

$$= 30{,}000\$ + 3000\$ + 600\$ = 33600\$ \text{ or } 4{,}170{,}768 \text{ birr}$$

Therefore the total investment cost for five DVR is 5*4,170,768 birr = 20,853,840 birr

Finally, 56,147,701.8 birr - 8,672,623.38 birr = 47,475,078.4224 birr/year or 382,462.566 $ utility can save from loss by implementing GOA based DVR.

The cost of return is determined based on expenses and profits, ultimately resulting in the rate of return being the time frame needed to recoup the investment costs. The calculation involves comparing the investment cost to the yearly savings generated at feeder line-6 (R4-G5) due to

the investment. Similarly, the calculation also involves comparing the purchase cost to the yearly savings generated at feeder line-6 (R4-G5) as a result of the investment.

$$\text{ROI} = \frac{\text{Investment value} - \text{Investment cost}}{\text{Investment cost}}$$

Where, ROI is return on investment, so $ROI = \frac{47{,}475{,}078.4224 - 20{,}853{,}840}{20{,}853{,}840} * 100$

= 1.276 or 127%.

A 127% ROI indicates that DVR installations are 1.276 times greater than the initial investment cost, highly cost-effective for Ethiopian electric utilities, likely due to severe existing losses and relatively low implementation costs.

Table 4. 11 Cost Analysis Result

Investment cost (ETB)	The annual savings in electricity costs from loss (ETB)
20,853,840	47,475,078.4224

4.10.1 Payback Period

The amount of months or years of benefits needed for the project to break even is known as the payback period. This approach establishes how long it takes to recoup the initial investment. Only when the payback period falls below a predetermined threshold established by the business is a project completed.

The following formula can be used to predict the payback period:

$$\text{Payback period} = \frac{\text{Investment cost}}{\text{annual savings in electricity costs from loss}}$$

$$= \frac{20{,}853{,}840}{47{,}475{,}078.4224}$$

Payback period= 6 month

Therefore, the time taken for the payback of the investment is approximately six month.

DVR can save a lot of money by minimizing downtime caused by voltage fluctuations and interruptions and avoiding damage to sensitive electrical equipment. This could lead to decreased energy use, lower maintenance and replacement costs, and more productivity. The one-month payback period indicates that the DVR's initial investment will be quickly returned in terms of money. This quick return on investment makes installing a single DVR on the distribution network is a very attractive to meet the main objective of the thesis as well as financial benefit of Ethiopian electric utility. The cost-benefit analysis of installing a DVR with a one-month payback period demonstrates that the investment is both financially possible and operationally useful for businesses looking to protect their equipment and guarantee a reliable power supply.

Chapter Five

Conclusion and Recommendation

5.1 Conclusion

This thesis is carried out on one of the Hawassa Feeder-6 (R4-G5) 15 kV distribution feeders utilizing distribution network analysis and MATLAB simulation. The purpose of power flow analysis is to ascertain the active and reactive power flows on the distribution lines, as well as the voltage magnitude and phase angle at each bus (node) in the system. Power quality disturbances are divided into four distinct wavelet filter levels using Debechesh-4 (Db-4). This enables the development of an approximate and comprehensive coefficient distribution in addition to the extraction of features such as the mean, maximum, and lowest values of the disturbances for power quality disruptions. The classification efficiency of neural networks and support vector machines (SVMs) is 100%. Lastly, a dynamic voltage restorer (DVR) combined with the Grasshopper Optimization Algorithm (GOA) can raise the voltage profile from 70% to 98.5% and lower the voltage swell from 110% to 98%, and also, based on applying different kinds of faults, easily test the voltage sag and swell by using DVR integrated with Wavelet transform algorithm. This reduces the possible influence on delicate systems and equipment while simultaneously enhancing the power supply's quality.

5.2 Recommendations

The following recommendations are based on this thesis work:

- Because of the growing loads and rising power demand, EEU and EEP should collaborate to use DVR to upgrade the current power distribution and transmission lines.
- In order to address future power quality issues, EEU must use CPD applications in power distribution lines.

5.3 Future Work

- Further research should focus on developing optimal placement algorithms for multiple Dynamic Voltage Restorers (DVRs) to mitigate different types of power quality disturbances in distribution and transmission networks.

Reference

[1] Alshahrani, Saeed Sultan. Detection, classification and control of power quality disturbances based on complementary ensemble empirical mode decomposition and artificial neural networks. Diss. Brunel University London, 2017.

[2] Mohammed, M. (2020). Investigation and Mitigation of Power Quality Problems (Case Study: ETUR Textile Factory) (Doctoral dissertation, ASTU).

[3] Bhagat, A., Nimkar, S., Dongre, K., & Ali, S. (2017). Power quality disturbance detection and classification using artificial neural network based wavelet. International Journal of Computational Intelligence Research, 13(8), 2043-2064.

[4] Kubendaran, A. K. P., Loganathan, A. K., & Cheren, S. E. (2020, March). Performance comparison of power quality improvement strategies for unified power quality conditioner in an interconnected distribution system. In 2020 Joint International Conference on Digital Arts, Media and Technology with ECTI Northern Section Conference on Electrical, Electronics, Computer and Telecommunications Engineering (ECTI DAMT & NCON) (pp. 180-185). IEEE.

[5] Eristi, B., Yildirim, O., Eristi, H., & Demir, Y. (2016, September). A real-time power quality disturbance detection system based on the wavelet transform. In 2016 51st International universities power engineering conference (UPEC) (pp. 1-5). IEEE.

[6] Haile, W. A., & Perumal, C. (2019). DETAILED ENERGY AUDIT OF AN INDUSTRIAL FIRM. A CASE STUDY OF ZUQUALLA STEEL ROLLING MILL (ZUSROM) FACTORY LOCATED IN DEBRE ZEIT TOWN, ETHIOPIA. Journal of Critical Reviews, 7(5), 2020.

[7] Jandan, F., Khokhar, S., Memon, Z., & Shah, S. (2019). Wavelet based simulation and analysis of single and multiple power quality disturbances. Engineering, Technology & Applied Science Research, 9(2), 3909-3914.

[8] Yeh, H. G., Sim, S., & Bravo, R. (2018, October). Symlets techniques for real time detection of transients generated by hif in the 12 kv distribution circuits. In 2018 IEEE Green Energy and Smart Systems Conference (IGESSC) (pp. 1-6). IEEE.

[9] Sarker, I. H. (2021). Machine learning: Algorithms, real-world applications and research directions. SN computer science, 2(3), 160.

[10] Praveen, J., Muni, B. P., Venkateshwarlu, S., & Makthal, H. V. (2004, November). Review of dynamic voltage restorer for power quality improvement. In 30th Annual Conference of IEEE Industrial Electronics Society, 2004. IECON 2004 (Vol. 1, pp. 749-754). IEEE.

[11] Jayasree, T., Devaraj, D., & Sukanesh, R. (2009). Power quality disturbance classification using S-transform and radial basis network. Applied Artificial Intelligence, 23(7), 680-693.

[12] Deepthi, K. (2019). Power quality assessment using change detection and DFT. International Journal of Recent Technology and Engineering (IJRTE), 8(1S3).

[13] Ilango, K., Bhargav, A., Trivikram, A., Kavya, P. S., Mounika, G., & Nair, M. G. (2012, December). Power quality improvement using STATCOM with renewable energy sources. In 2012 IEEE 5th India international conference on power electronics (IICPE) (pp. 1-6). IEEE.

[14] Anjaiah, K., & Patnaik, R. K. (2019). An advanced signal processing based multiclass power quality disturbance detection and classification technique for grid connected solar PV farm. International Journal of Innovative Technology and Exploring Engineering, 8(9), 876-896.

[15] Girón, C., Rodríguez, F. J., de Urtasum, L. G., & Borroy, S. (2018). Assessing the contribution of automation to the electric distribution network reliability. International Journal of Electrical Power & Energy Systems, 97, 120-126.

[16] Anteneh, D., Khan, B., Mahela, O. P., Alhelou, H. H., & Guerrero, J. M. (2021). Distribution network reliability enhancement and power loss reduction by optimal network reconfiguration. Computers & Electrical Engineering, 96, 107518.

[17] Hamour, H., Kamel, S., Abdel-mawgoud, H., Korashy, A., & Jurado, F. (2018, September). Distribution network reconfiguration using grasshopper optimization algorithm for power loss minimization. In 2018 International Conference on Smart Energy Systems and Technologies (SEST) (pp. 1-5). IEEE.

[18] Dursun, I., Karaosmanoglu, F., & Umurkan, N. (2016). Reconfiguration of actual distribution network with optimum power flow for loss reduction. International Journal of Electronics and Electrical Engineering, 4(1), 56-60.

[19] Narkvichian, P., & Oonsivilai, A. (2017). Optimal selection switching of remote terminal unit using reliability index in electric power distribution systems. Energy Procedia, 138, 128-133.

[20] Sadeghi, M., & Kalantar, M. (2023). Fully decentralized multi-agent coordination scheme in smart distribution restoration: Multilevel consensus. Applied Energy, 350, 121606.

[21] Najafi, J., Peiravi, A., & Guerrero, J. M. (2018). Power distribution system improvement planning under hurricanes based on a new resilience index. Sustainable cities and society, 39, 592-604.

[22] Li, B., Wei, J., Liang, Y., & Chen, B. (2020). Optimal placement of fault indicator and sectionalizing switch in distribution networks. IEEE Access, 8, 17619-17631.

[23] Ahmadigorji, M., Amjady, N., & Dehghan, S. (2017). A novel two-stage evolutionary optimization method for multiyear expansion planning of distribution systems in presence of distributed generation. Applied Soft Computing, 52, 1098-1115.

[24] Sedighizadeh, M., Esmaili, M., & Mahmoodi, M. M. (2017). Reconfiguration of distribution systems to improve re-liability and reduce power losses using imperialist com-petitive algorithm. Iranian Journal of Electrical & Electronic Engineering, 13(3), 287.

[25] Barghi Latran, M., Teke, A., & Yoldaş, Y. (2015). Mitigation of power quality problems using distribution static synchronous compensator: a comprehensive review. IET power electronics, 8(7), 1312-1328.

[26] Alam, M. R., Bai, F., Yan, R., & Saha, T. K. (2020). Classification and visualization of power quality disturbance-events using space vector ellipse in complex plane. IEEE Transactions on Power Delivery, 36(3), 1380-1389.

[27] Xie, J., Chen, C., & Long, H. (2021). A loss reduction optimization method for distribution network based on combined power loss reduction strategy. Complexity, 2021(1), 9475754.

[28] Ahsan, M. K., Pan, T., & Li, Z. (2018). A three decades of marvellous significant review of power quality events regarding detection & classification. Journal of Power and Energy Engineering, 6(8), 1-37.

[29] Okelola, M. O. (2015). Detection and Classification of Power Quality Events Using Discrete Wavelet Transform and Support Vector Machine. International Journal of Engineering Research and Technology, 4(6), 338-342.

[30] Balakumar, S., Getahun, A., Kefale, S., & Kumar, K. R. (2021). Improvement of the voltage profile and loss reduction in distribution network using moth flame algorithm: Wolaita Sodo, Ethiopia. Journal of Electrical and Computer Engineering, 2021(1), 9987304.

[31] Ray, P. K., Dash, S. K., Subudhi, B., & Korkua, S. K. (2020). Mitigation of power quality issues using UPQC. International Journal of Emerging Electric Power Systems, 21(5), 20200040.

[32] Saremi, S., Mirjalili, S., & Lewis, A. (2017). Grasshopper optimization algorithm: theory and application. Advances in engineering software, 105, 30-47.

[33] Saremi, S., Mirjalili, S., & Lewis, A. (2017). Grasshopper optimization algorithm: theory and application. Advances in engineering software, 105, 30-47.

[34] Taye, T. (2019). Improvement of Distribution Feeder Loss and Voltage Profile (Case Study: Bella Substation Distribution Feeder). Addis Ababa University, Addis Ababa, Ethiopia.

[35] Mohammed, H., Khan, F. A., & Abubeker, W. (2022). POWER QUALITY ANALYSIS OF AN ELECTRIC DISTRIBUTION SYSTEM USING ANN-CONTROLLED DVR (Doctoral dissertation, Haramaya University).

Appendix

Line data and load data for load flow analysis:

From	To	R	X	P(KW)	Q(KVAR)
1	2	0.391	0.766	97.97	40.4
2	3	0.852	0.159	60.91	39.08
3	4	0.827	0.562	66.89	36.18
4	5	0.826	0.641	55.66	33.15
5	6	0.847	0.052	30.44	8.34
6	7	0.789	0.755	69.1	41.49
7	8	0.627	0.694	151.4	88.3
8	9	0.492	0.295	220.5	140.7
9	10	0.434	0.26	294.2	147.3
10	11	0.487	0.052	196.1	103.6
11	12	0.694	0.416	55.66	33.15
12	13	0.636	0.382	0.382	107.1
13	14	0.289	0.174	128.7	70.3
14	15	0.694	0.416	140.6	77.58
15	16	0.764	0.458	209	123.6
16	17	0.412	0.447	99.2	52.3
17	18	0.412	0.847	151.4	78.3
18	19	0.202	0.121	129.5	70.81
19	20	0.174	0.104	219.3	105.6
20	21	0.706	0.423	99.2	62.3
9	22	0.683	0.409	97.89	52
22	23	0.318	0.191	197.1	100.9
23	24	0.868	0.521	231.4	158.7
24	25	0.678	1.006	13.21	10.75
25	26	0.883	0.406	244.6	157.3
15	27	0.434	0.26	90.02	49.47
27	28	0.411	0.246	183.12	72.99
28	29	0.289	0.174	93.1	87.04
29	30	0.341	0.205	276.22	123.6
30	31	0.388	0.433	206.1	108.4
31	32	0.099	0.159	64	37.64
32	33	0.159	0.295	44.8	15.07
33	34	0.997	0.797	128.9	74.4
34	35	0.378	0.426	64.45	32.2
35	36	0.058	0.035	164.1	107.1
36	37	0.058	0.035	65.64	36.84
37	38	0.418	0.45	210.7	124.3

38	39	0.349	0.409	359.4	282.6
48	40	0.163	0.697	148.7	86.6
40	41	0.064	0.638	52.6	24.59
41	42	0.893	0.735	157.8	51.67
42	43	0.25	0.75	189.2	85.3
43	44	0.33	0.198	14	7.09
44	45	0.359	0.815	31.82	26.18
45	46	0.636	0.621	16.43	7.59
46	47	0.576	0.645	56.14	41.1
47	48	0.33	0.198	72.57	48.69
40	49	0.145	0.087	126.32	100.4
49	50	0.388	0.833	107.5	73.3
50	51	0.908	0.545	27.28	21.81
51	52	0.875	0.725	267.28	157.9
52	53	0.586	0.551	240	102.3
53	54	0.503	0.302	60	40.85
54	55	0.14	0.284	93.7	31.35
55	56	0.159	0.895	127.4	109.2
56	57	0.659	0.396	63.7	54.6
57	58	0.422	0.253	175.7	57.15
58	59	0.163	0.697	112	99.5
59	60	0.972	0.583	38.4	12.73
54	61	0.174	0.104	72	32.63
61	62	0.55	0.33	67.2	25.78
62	63	0.753	1.051	25.78	22.88
63	64	0.48	0.288	128.9	74.4
64	65	0.868	0.521	31.56	23.07
65	66	0.278	0.767	36.78	11.56
66	67	0.431	0.658	58	32.46
67	68	0.507	0.642	28.8	20.23
61	69	0.463	0.278	124.1	81.7
69	70	0.679	0.547	93.51	61.9
70	71	0.996	0.197	114.47	92.28
71	72	0.978	0.187	11.21	9.35
72	73	0.975	0.984	93.8	58.3
73	74	0.989	0.593	19.46	11.81
74	75	0.979	0.947	65.24	25.84
75	76	0.831	0.898	80.64	24.3

DVR System Data

No.	System quantities	Ratings
1	Main supply voltage per phase and frequency	15kv,50hz
2	Injection transformer turn ratio	1:1
3	Dc bus voltage	700v
4	Inductance	0.344 mH
5	Capacitance	0.57F
6	DVR size	100kva

Base case load flow code

```
function [V_basecase,PL_basecase,QL_basecase] = LoadflowBase()
global d V- base
from_bus = d(:,1);
to_bus = d(:,2);
r = d(:,3);
x = d(:,4);
z = complex(r,x);
no_branch = length(d(:,1));
no_bus = max(max(d(:,1:2)));
V_bus = V_base*ones(no_bus,1);
PD = zeros(no_bus,1);
```

```
QD = zeros(no_bus,1);
PDG = zeros(no_bus,1);
S_base = 20000;
Z_base = V_base^2/S_base;
S = zeros(no_bus,1);
I_bus = zeros(no_bus,1);
for a = 1:no_branch
    b = to_bus(a);
    PD(b) = (d(a,5)*1e3);
    QD(b) = (d(a,6)*1e3);
    S(b) = complex(PD(b),QD(b));
end
tol = inf;
iter = 1;
while tol > 1e-10 && iter < 50

    for a = 1:no_branch
        b = to_bus(a);
        I_bus(b) = conj(S(b)/V_bus(b));
    end
    I_branch = zeros(no_branch,1);
    for a = no_branch:-1:1
        b = to_bus(a);
        for c = 1:no_branch
            if b == from_bus(c)
```

```
            I_branch(a) = I_branch(a) + I_branch(c);
        end
    end
    I_branch(a) = I_branch(a) + I_bus(b);
end
for a = 1:no_branch
    b = from_bus(a);
    c = to_bus(a);
    V_bus(c) = V_bus(b) - z(a)*I_branch(a);
end
Scalc = V_bus.*conj(I_bus);
Sflow  = 1e-3*(V_bus(1:end-1).*conj(I_branch(:,1:end)));
Sloss  = conj(I_branch.^2.*z)*1e-3;
tol = max(abs(real(Scalc) - real(S)));
iter = iter + 1;
end
S_inj(1) = V_bus(1)*conj(I_branch(1));
P(1) = real(S_inj(1)); Q(1) = imag(S_inj(1));
Pkw = P;  Qkw = Q;
LP = sum(real(Sloss)); %Pkw(1)-sum(PD);
LQ = sum(imag(Sloss)); %Qkw(1)-sum(QD);
Ploss = LP; Qloss = LQ;
V = V_bus./V_base;
Vang = angle(V_bus);
V_basecase = abs(V)';
```

```
PL_basecase = real(Sloss);

QL_basecase = imag(Sloss);

PL = real(Sloss); QL = abs(imag(Sloss));

[Vmin,VminBus]=min(V_basecase);

% disp('       Bus Voltage Profile         ')

% disp('-----------------------------------')

% disp('  Bus    Vbus(pu)  Angle(deg)')
```

Fault in power system using wavelet transform integrated with DVR simulink

```
Clc;

Clear all;

Open ('faultdet.slx'.);

Sim ('faultdet.slx'.);

Current A = current 1;

Current B = current 2;

Current C = current 3;

Current G = current 4;

[CA, LA] = wavedec (current A, 1, 'db4');

[CB, LB] = wavedec (current B, 1, 'db4');

[CC, LC] = wavedec (current C, 1, 'db4');

[CG, LG] = wavedec (current G, 1, 'db4');

Coef A = detcoef (cA, LA, 1);

Coef B = detcoef (cB, LB, 1);

Coef C = detcoef (cC, LC, 1);

Coef G = detcoef (cG, LG, 1);

m = max (coefA)
```

```
n = max (coefB)
p = max (coefC)
q = max (coefG)
If m > 200
   If n > 200
      If p > 200
         If q > 200
Disp ("Three Phase to ground Fault is detected")
      End
   End
   End
End
If m > 200
   If n > 200
      If p > 200
         If q < 200
Disp ("Three Phase Fault is detected")
      End
   End
   End
End
If m > 200
   If n > 200
      If p < 200
         If q > 200
```

```
Disp ("Double Line to Gournd Fault (AB-G) is detected")
        End
    End
    End
End
If m > 200
    If n < 200
        If p > 200
            If q > 200
Disp ("Double Line to Gournd Fault (AC-G) is detected")
        End
    End
    End
End
If m < 200
    If n > 200
        If p > 200
            If q > 200
Disp ("Double Line to Gournd Fault (BC-G) is Detected")
        End
    End
    End
End
If m > 200
    If n > 200
```

```
        If p < 200
            If q < 200
Disp ("Line to Line Fault between Phase A and B is detected")
        End
    End
    End
End
If m > 200
    If n < 200
        If p > 200
            If q < 200
Disp ("Line to Line Fault between Phase A and C is detected")
        End
    End
    End
End
If m < 200
    If n > 200
        If p > 200
            If q < 200
Disp ("Line to Line Fault between Phase B and C is detected")
        End
    End
    End
End
```

```
If m > 200
    If n < 200
        If p < 200
            If q > 200
Disp ("Single Line to Ground Fault in Phase A is detected")
        End
    End
    End
End
If m < 200
    If n > 200
        If p < 200
            If q > 200
Disp ("Single Line to Ground Fault in Phase B is detected")
        End
    End
    End
End
If m < 200
    If n < 200
        If p > 200
            If q > 200
Disp ("Single Line to Ground Fault in Phase C is detected")
        End
    End
```

```
    End
End
If m < 200
    If n < 200
        If p < 200
            If q < 200
Disp ("No Fault is detected. System is Normal")
        End
    End
    End
End
```